

A Universal Evolution Equation for Elastic Scattering: Bridging Elastic Scattering and Small-x Dynamics

Anderson Kendi Kohara

Ecole Polytechnique – Palaiseau - France



Iceland
Liechtenstein
Norway grants

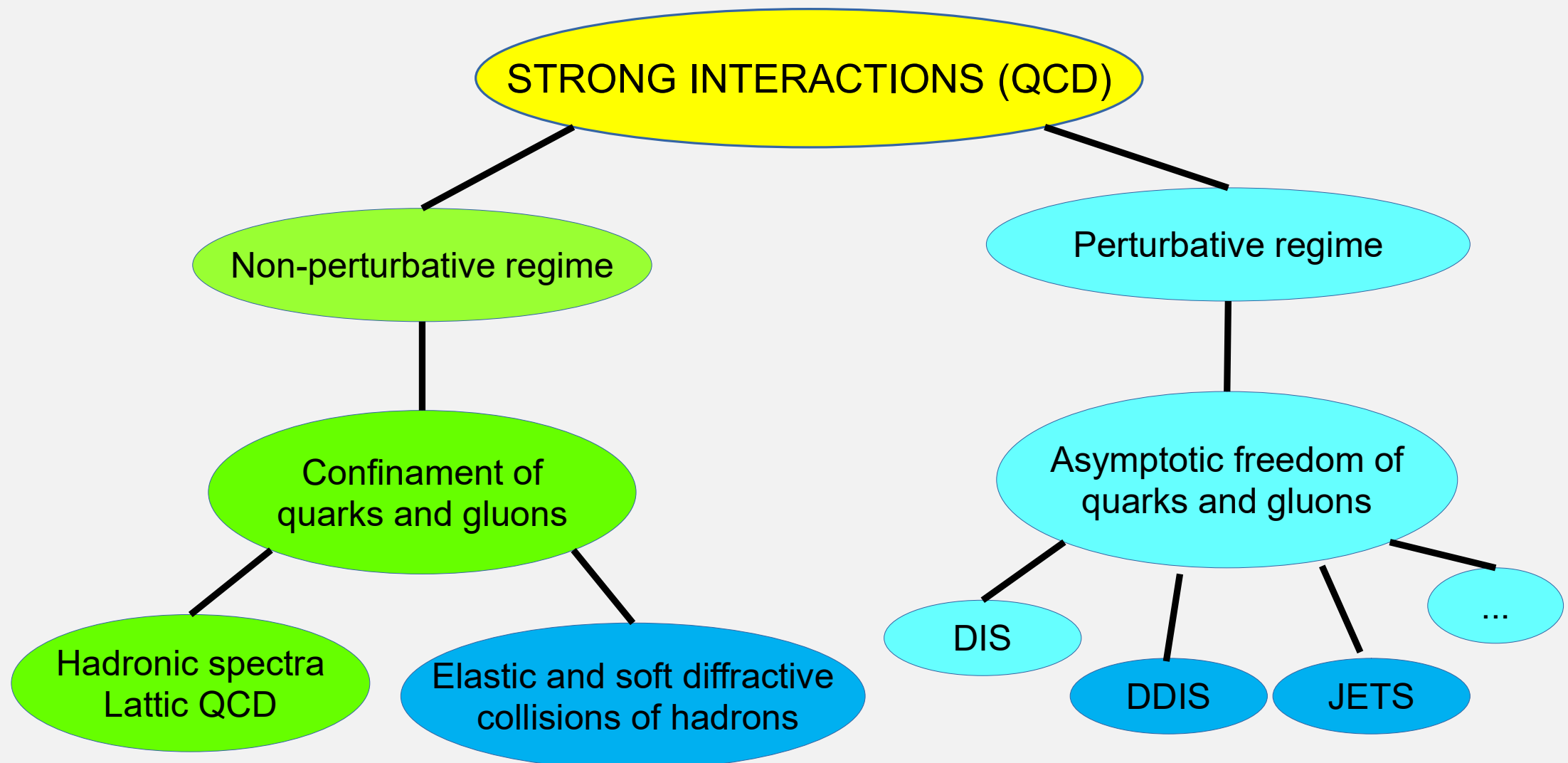


IP2I

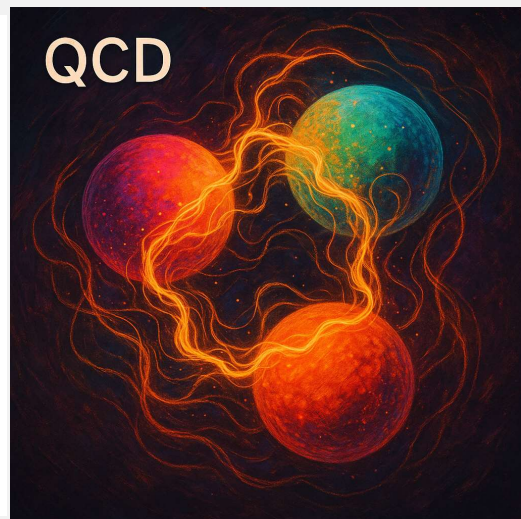
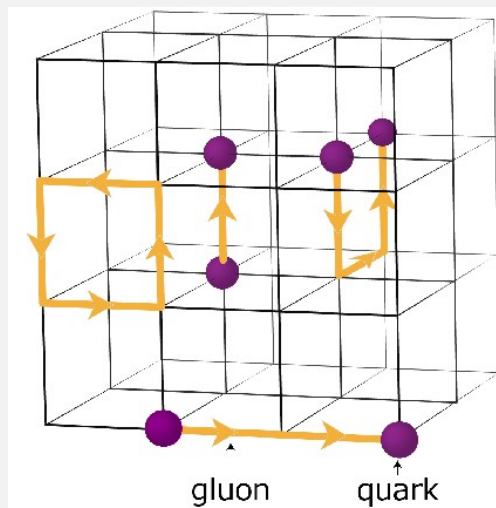
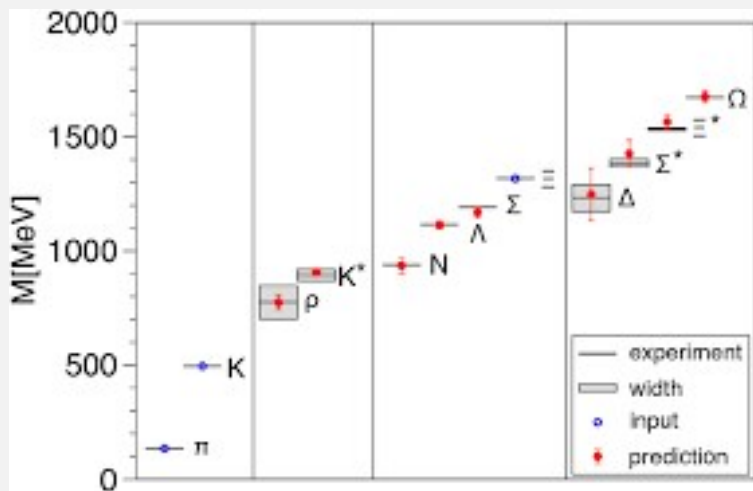
June 23, 2025



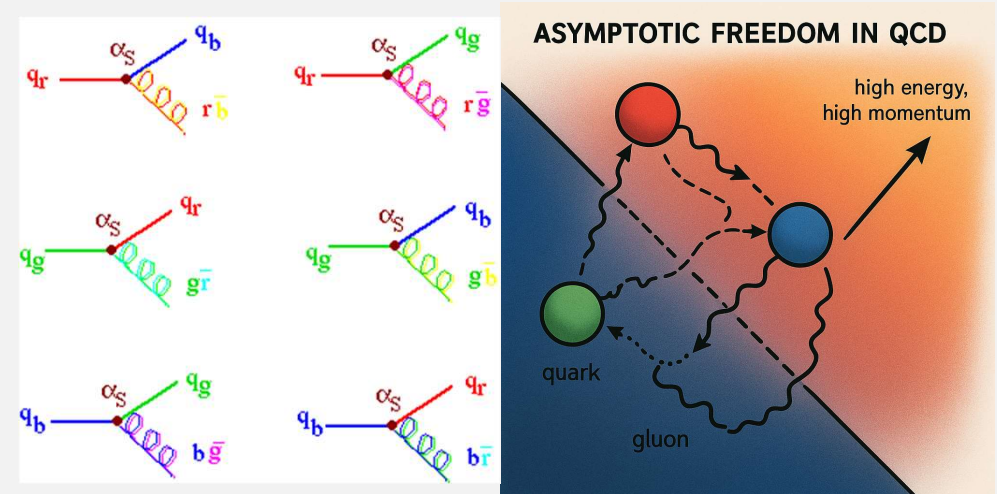
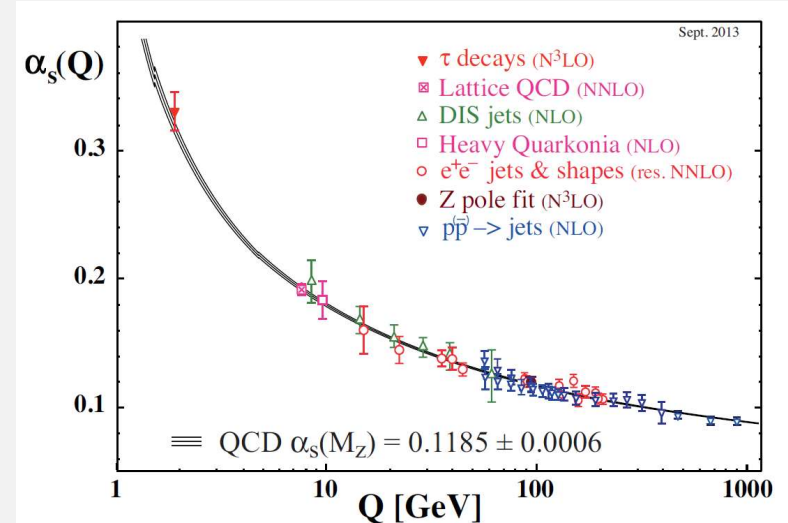
Preliminary discussions



Confinement



Asymptotic freedom

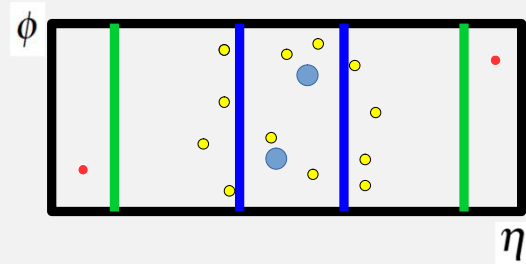


$$Z = \int D U e^{-s[U]} ; \langle O \rangle = \frac{1}{Z} \int D U \, O(U) e^{-s[U]}$$

$$\mathcal{L}_{QCD} = \bar{\psi} (i \not{D} T_a - m) \psi - \frac{1}{4} F_a^{\mu\nu} F_{\mu\nu}^a$$

Elastic scattering is a diffractive process

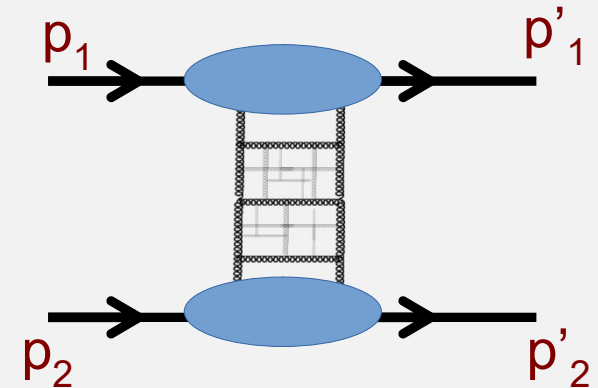
- **Experimental point of view**
- Diffractive peak in forward regime
- Rapidity gaps: pseudo rapidity *versus* azimuthal angle



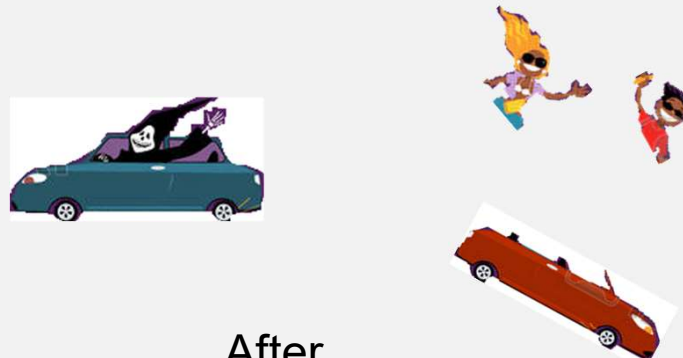
- **Theoretical point of view**
- Initial and final states have the same quantum numbers
- (Pomeron exchange)



Before



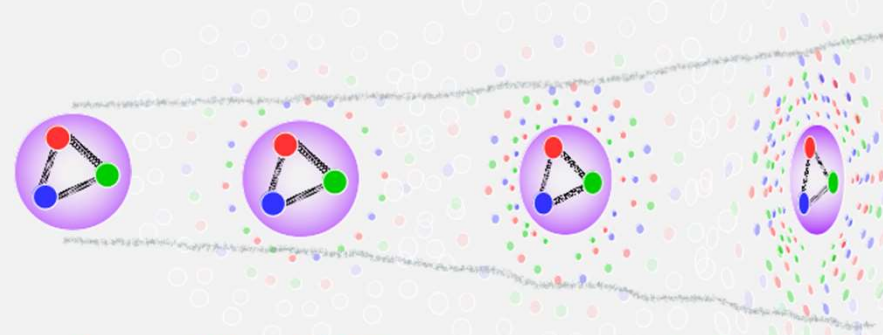
After



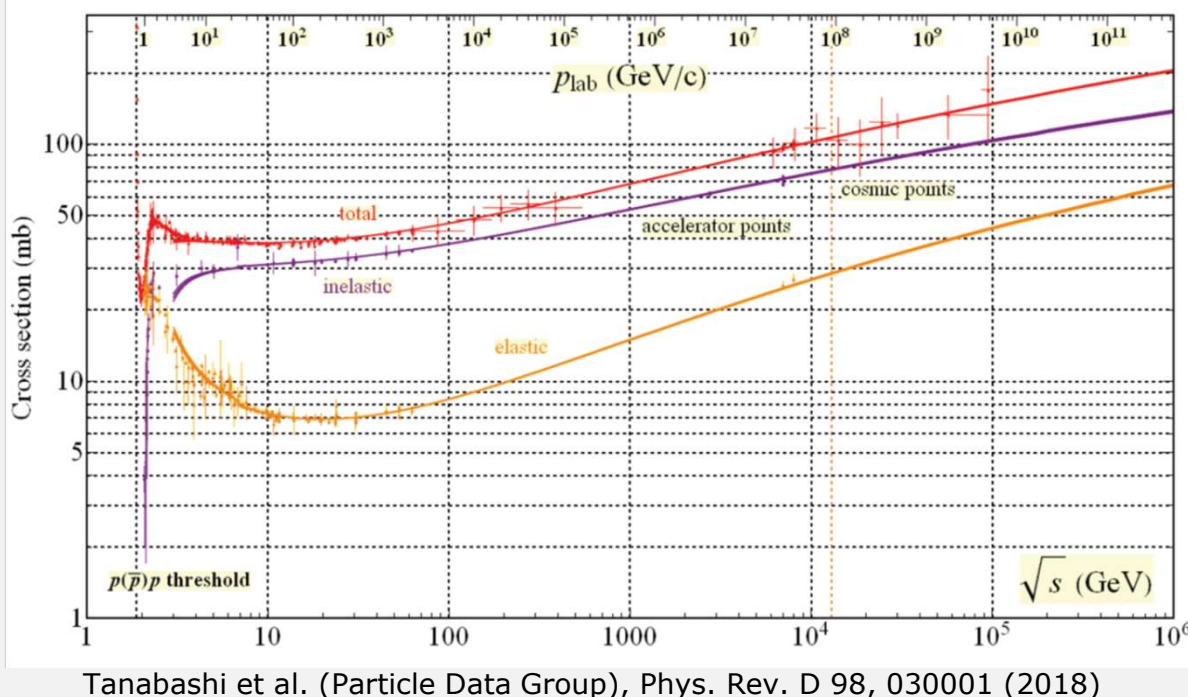
Introduction

- Elastic scattering is a diffractive phenomenon
- The particles remain intact, changing direction
- Crucial for probing the geometry of hadrons.
- Unitarization effects at high energies
- Interplay between Coulomb interaction and strong force

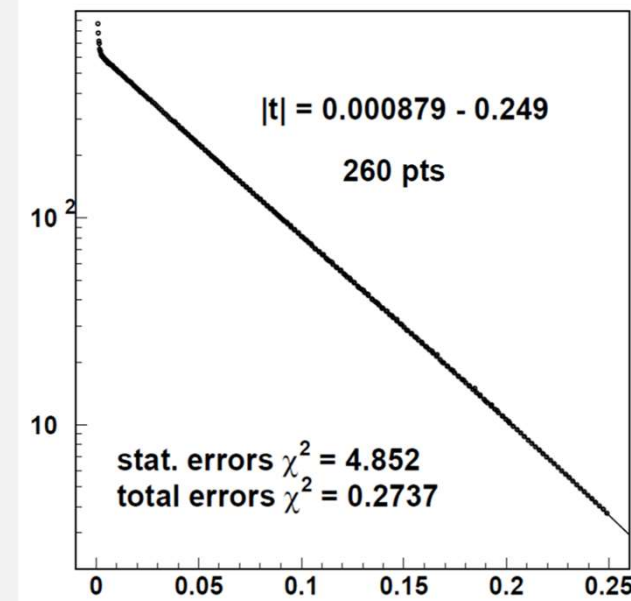
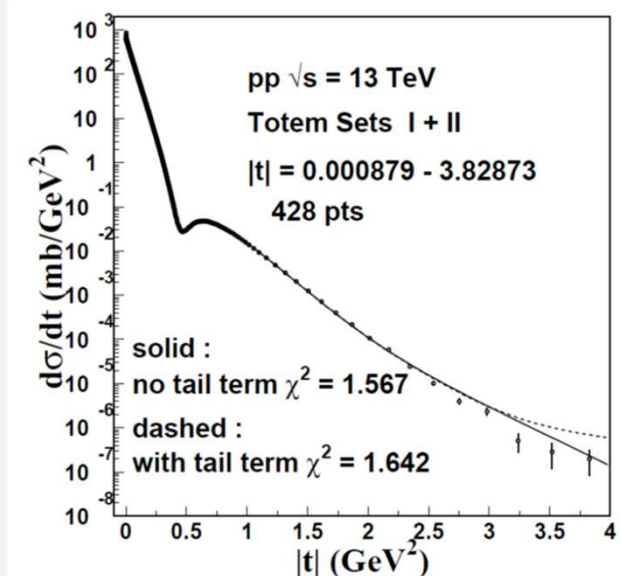
integrated cross sections – energy dependent



Observation of the QCD vacuum excitation with the energy Energy



differential cross section – fixed energy t^2



A. K. K., E. Ferreira, and T. Kodama., Eur. Phys. J. C, 74 (2014)

Basic physical quantities are observed in t momentum space

Forward quantities $t = 0$

Optical theorem $\sigma_{to} = 4\pi(\hbar c)^2 T_I^N(s, t = 0)$

Ratio of real and imaginary amplitudes $\rho = \frac{T_R^N(s, t = 0)}{T_I^N(s, t = 0)}$

And the slope

$$B = \left. \frac{d}{dt} \log \frac{d\sigma}{dt} \right|_{t=0}$$

Differential cross section

$$\frac{d\sigma}{dt} = |T(s, t)|^2$$

Some challenges:

- Seemingly simple kinematics but complicated dynamics
- Non-perturbative phenomenon
- Long range force interplays with short ranged
- Experimental gap among energies
- Differential cross sections with fluctuations (and/or) large uncertainties
- Lack of cross-symmetric experiments at the same energies

Hadronic Collider Experiments

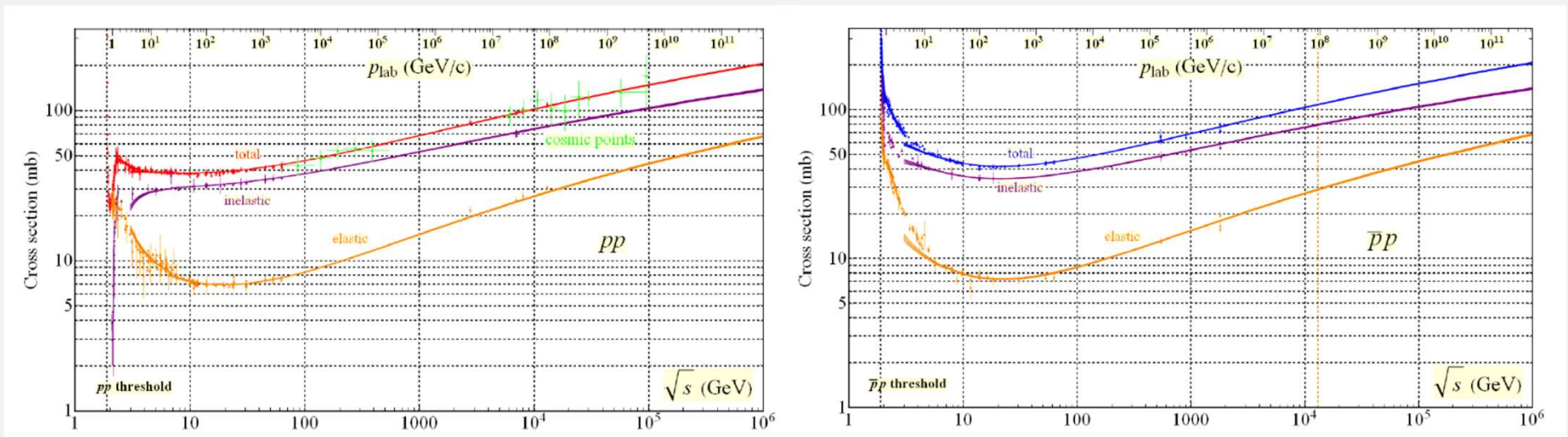
Intersecting Storage Rings-CERN, 1971–1984

Proton-Antiproton Collider(SPS)-CERN, 1981–1991

Tevatron-Fermilab, 1987–2011

Relativistic Heavy Ion Collider-BNL, 2000–...

Large Hadron Collider-CERN, 2009–...



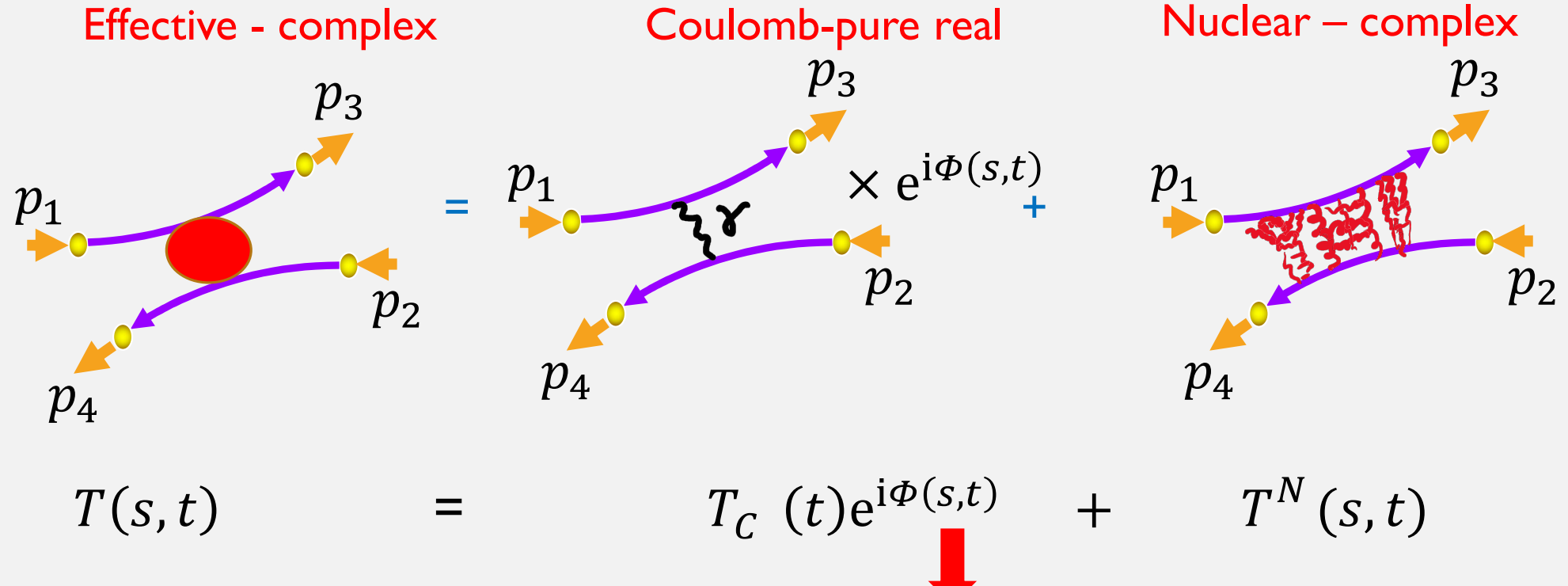
Interesting problems:

- It is the most basic diffractive phenomenon at high energies.
- It is vacuum interaction.
- What is the Pomeron and how many of them?
- What is the odderon? Does it exist?
- Several different models, but is there an equation to describe it?
- What is the connection of this physics and the QCD?
- How strong and electromagnetic forces interplay?

Important high energy theorems and hypotheses

- Unitarity $\sigma_{tot} = \sigma_{el} + \sigma_{inel}$ or $0 \leq \text{Im } \tilde{T}(s, b) \leq 1$
- Froissart bound
(strong force short ranged) $\sigma_{tot}(\tau(s) \rightarrow \infty) \leq C\tau^2 = C \log^2 s$
- Dispersion relations $\text{Re } T(s, t = 0) = \frac{1}{\pi} P \int_{-\infty}^{\infty} \frac{\text{Im } T(s', t = 0)}{s' - s} ds'$
- Martin's zero $\text{Re } T(s, t_0) = 0$ at some point for a small t_0
- Crossing symmetry $T_{pp}(s, t, u) = T_{p\bar{p}}(u, t, s)$

Relativistic elastic scattering



Mandelstam variables

$$s = (p_1 + p_2)^2$$

$$t = (p_1 - p_3)^2$$

$$u = (p_1 - p_4)^2$$

Coulomb phase –forward scattering– a long story...

- L.D. Solov'ev, JETP **22**, 205 (1966) 26;
 H. Bethe, Ann. Phys. (N.Y.) **3**, 190 (1958) 27;
 G.B. West, D.R. Yennie, Phys. Rev. **172**(5), 1413 (1968);
 V. Kundrat and M. Lokajcek, Phys. Lett. B **611** (2005) 102;
 R. Cahn, Z. Phys. C **15** (1982) 253.

Some models of elastic scattering amplitudes

$$T^N(s, t) = T_R^N(s, t) + iT_I^N(s, t)$$

- Bourrely Soffer Wu (eikonalized model based on crossing symmetry properties)
- Kohara Ferreira Kodama (based on stochastic vaccum model)
- Donnachie Landshoff (double Pomeron exchange + “perturbative tri-gluon exchange”)
- DGM (dinamical gluon mass)
- Jenkovszky model (Regge based)
- Białas Bzdak (Glauber based)
- HEGS ()
- ...

If you want to, you can increase this list

...

From *t*-space to *b*-space

We need to Fourier transform the scattering amplitude from *t* to *b* space

$$\tilde{T}(s, b) = i \int d^2 q e^{iq \cdot b} T(s, q^2)$$

Physical cross sections are written

$$\sigma_{el}(s) = \int d^2 \vec{b} \left| \tilde{T}(s, \vec{b}) \right|^2 = \int d^2 \vec{b} \frac{d\tilde{\sigma}_{el}}{d^2 \vec{b}}(s, \vec{b})$$

$$\sigma_{tot}(s) = 2 \int d^2 \vec{b} \tilde{T}_I(s, \vec{b}) = \int d^2 \vec{b} \frac{d\tilde{\sigma}_{tot}}{d^2 \vec{b}}(s, \vec{b})$$

$$\sigma_{inel}(s) = \int d^2 \vec{b} G_{inel}(s, \vec{b}) = \int d^2 \vec{b} \frac{d\tilde{\sigma}_{inel}}{d^2 \vec{b}}(s, \vec{b})$$

Unitarity constraint in *b* space

$$\sigma_{tot} = \sigma_{el} + \sigma_{inel}$$



Assuming independent $d^2 \vec{b}$ increments

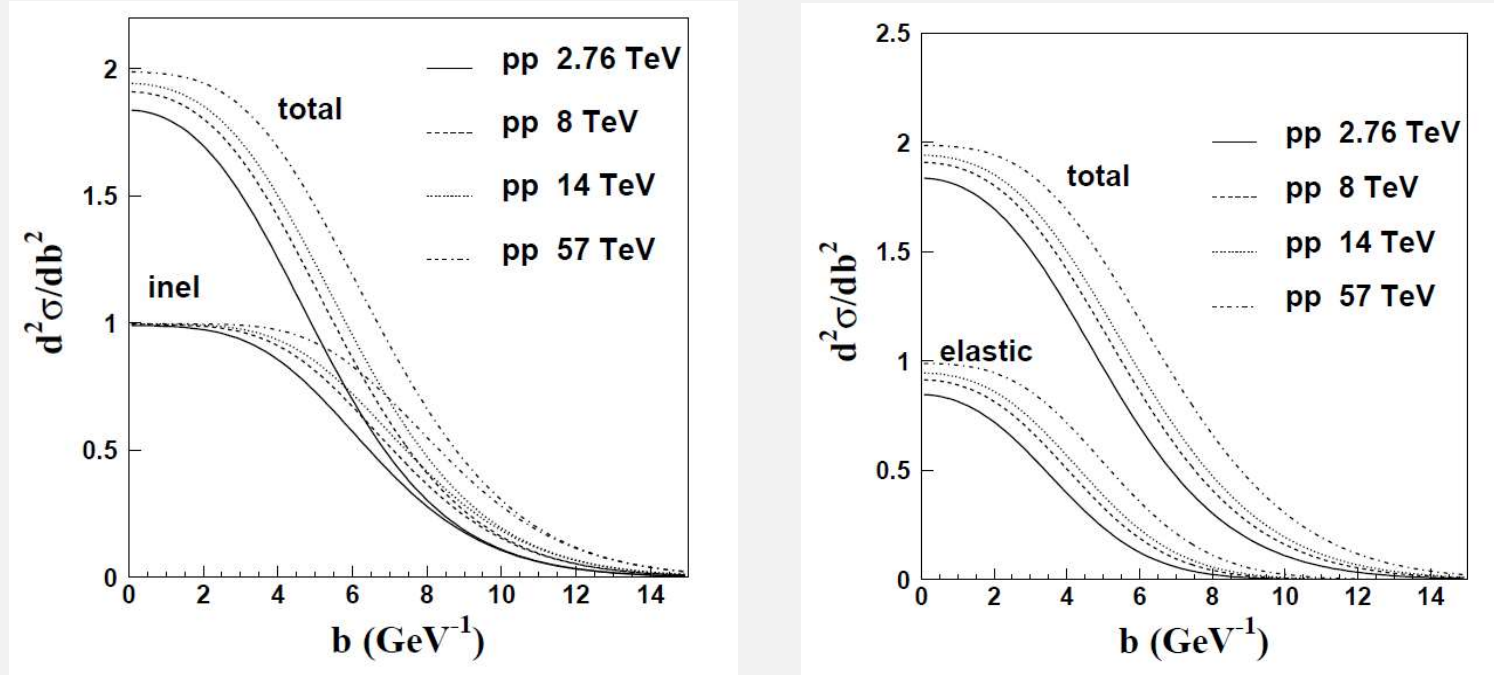
$$2 \tilde{T}_I(s, b) = |\tilde{T}(s, b)|^2 + G_{inel}(s, b)$$

$$G_{inel}(s, b) \approx \tilde{T}_I(s, b)[2 - \tilde{T}_I(s, b)] - \tilde{T}_R(s, b)^2$$

0

$$G_{inel}(s, b) \leq 1$$

Monotonic results for elastic differential 'cross sections' profile functions



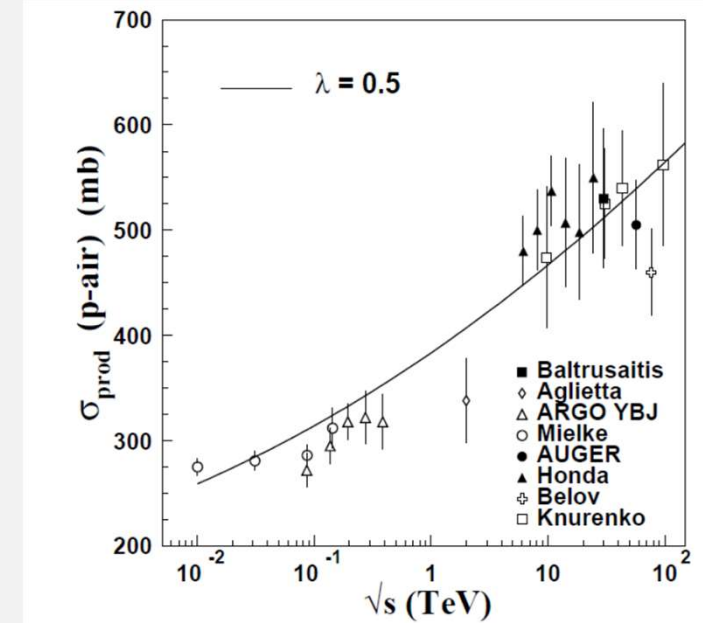
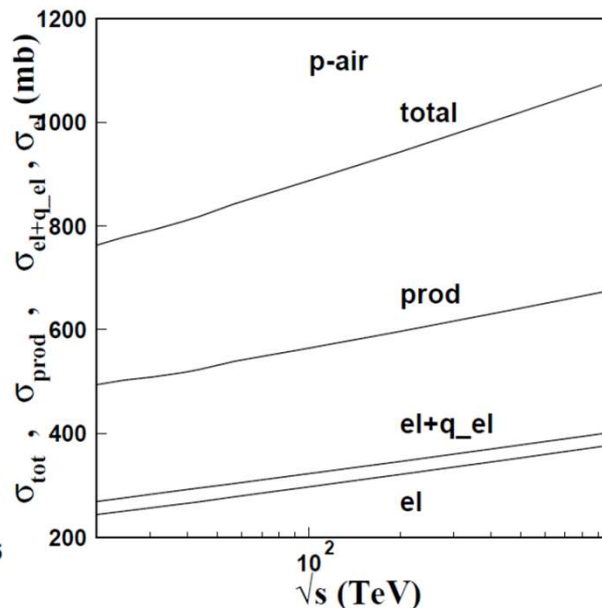
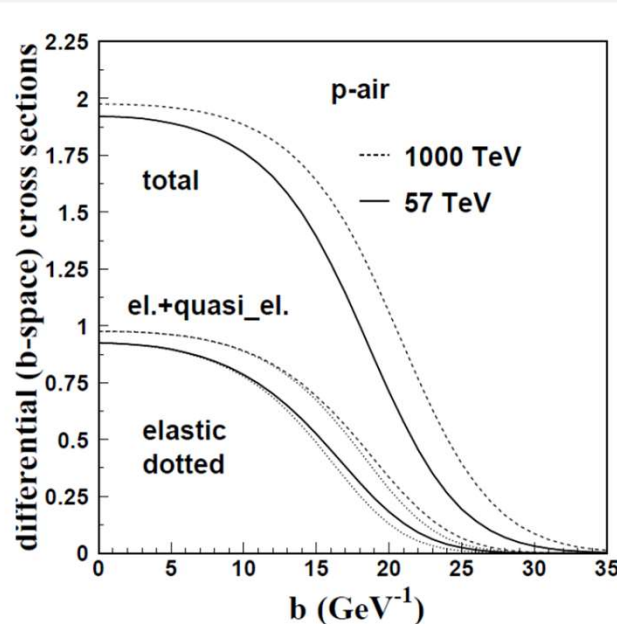
A. K. K., E. Ferreira, and T. Kodama., Eur. Phys. J. C, 74 (2014)

- Interesting diffusive behaviour with increasing energy
- Unitarity bound saturation

This geometrical space allows extrapolations to larger targets

Using Glauber method we obtain pAir from pp

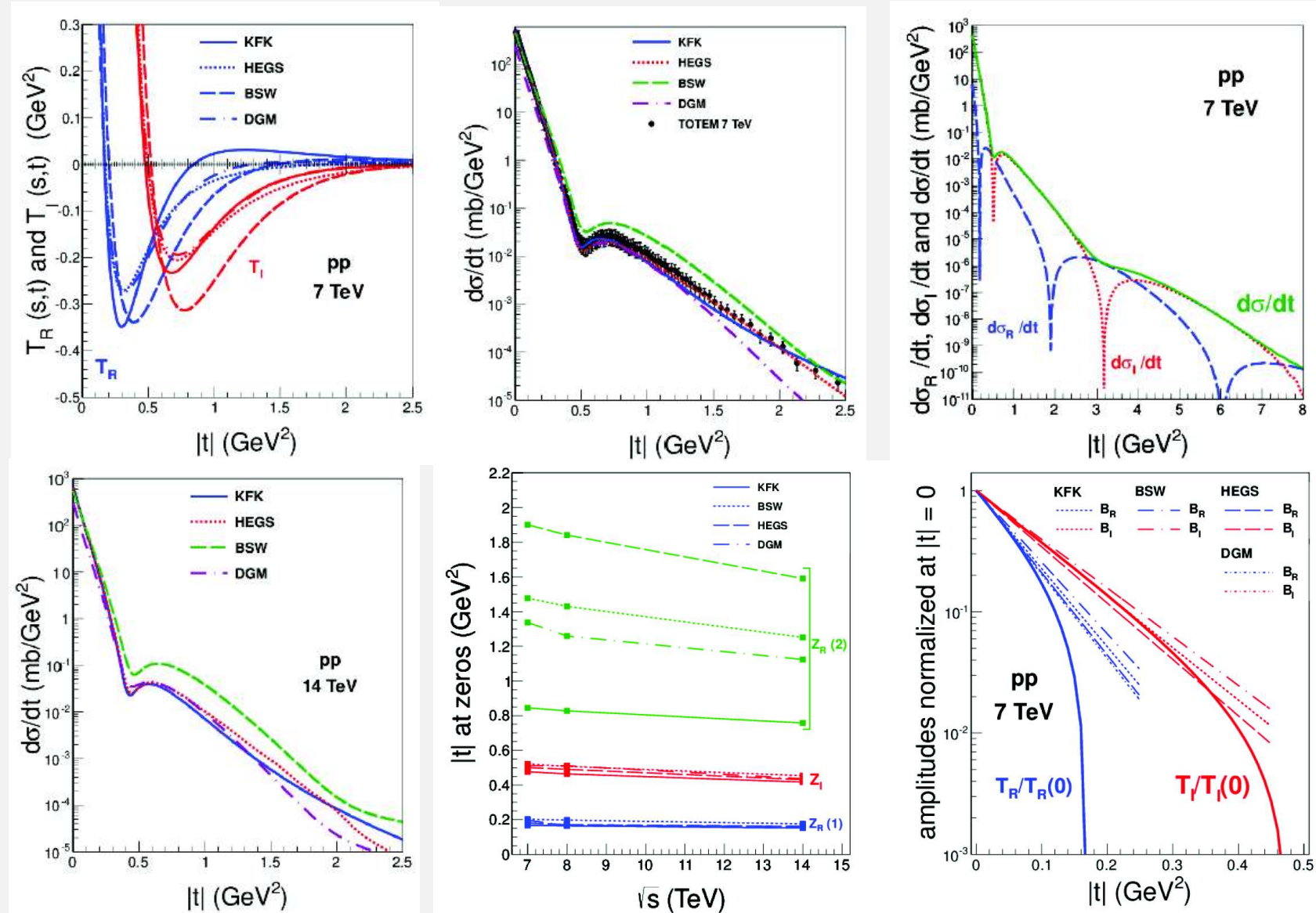
R.J. Glauber, Phys. Rev. 100 (1955) 242–248;
 R.J. Glauber and G. Matthiae, Nucl. Phys. B21(1970) 135–157.



A. K. K., E. Ferreira, and T. Kodama., J. Phys. G 41 (2014) 11, 115003

- Diffusive behaviour still holds with increasing energy
- Unitarity bound saturation still holds

Different models: amplitudes, differential cross sections, zeros, slopes



Fitting an elephant

Drawing an elephant with four complex parameters

Jürgen Mayer

Max Planck Institute of Molecular Cell Biology and Genetics, Pfotenhauerstr. 108, 01307 Dresden, Germany

Khaled Khairy

European Molecular Biology Laboratory, Meyerhofstraße, 1, 69117 Heidelberg, Germany

Jonathon Howard

Max Planck Institute of Molecular Cell Biology and Genetics, Pfotenhauerstr. 108, 01307 Dresden, Germany

A turning point in Freeman Dyson's life occurred during a meeting in the Spring of 1953 when Enrico Fermi criticized the complexity of Dyson's model by quoting Johnny von Neumann:¹ "With four parameters I can fit an elephant, and with five I can make him wiggle his trunk." Since then it has become a well-known saying among physicists, but nobody has successfully implemented it.

To parametrize an elephant, we note that its perimeter can be described as a set of points $(x(t), y(t))$, where t is a parameter that can be interpreted as the elapsed time while going along the path of the contour. If the speed is uniform, t becomes the arc length. We expand x and y separately² as a Fourier series

$$x(t) = \sum_{k=0}^{\infty} (A_k^x \cos(kt) + B_k^x \sin(kt)), \quad (1)$$

$$y(t) = \sum_{k=0}^{\infty} (A_k^y \cos(kt) + B_k^y \sin(kt)), \quad (2)$$

where A_k^x , B_k^x , A_k^y , and B_k^y are the expansion coefficients. The lower indices k apply to the k th term in the expansion, and the upper indices denote the x or y expansion, respectively.

Using this expansion of the x and y coordinates, we can analyze shapes by tracing the boundary and calculating the coefficients in the expansions (using standard methods from Fourier analysis). By truncating the expansion, the shape is smoothed. Truncation leads to a huge reduction in the information necessary to express a certain shape compared to a pixelated image, for example. Székely *et al.*³ used this approach to segment magnetic resonance imaging data. A similar approach was used to analyze the shapes of red blood cells,⁴ with a spherical harmonics expansion serving as a 3D generalization of the Fourier coordinate expansion.

The coefficients represent the best fit to the given shape in the following sense. The $k=0$ component corresponds to the center of mass of the perimeter. The $k=1$ component corresponds to the best fit ellipse. The higher order components

trace out elliptical corrections analogous to Ptolemy's epicycles.⁵ Visualization of the corresponding ellipses can be found at Ref. 6.

We now use this tool to fit an elephant with four parameters. Wei⁷ tried this task in 1975 using a least-squares Fourier sine series but required about 30 terms. By analyzing the picture in Fig. 1(a) and eliminating components with amplitudes less than 10% of the maximum amplitude, we obtained an approximate spectrum. The remaining amplitudes were

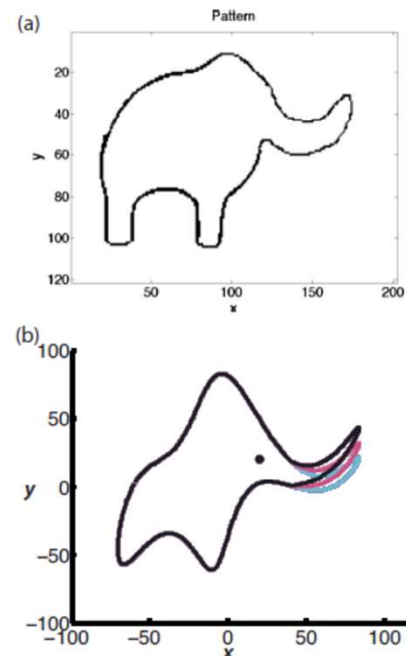


Fig. 1. (a) Outline of an elephant. (b) Three snapshots of the wiggling trunk.

Table I. The five complex parameters p_1, \dots, p_5 that encode the elephant including its wiggling trunk.

Parameter	Real part	Imaginary part
$p_1 = 50 - 30i$	$B_1^x = 50$	$B_1^y = -30$
$p_2 = 18 + 8i$	$B_2^x = 18$	$B_2^y = 8$
$p_3 = 12 - 10i$	$A_3^x = 12$	$A_3^y = -10$
$p_4 = -14 - 60i$	$A_4^x = -14$	$A_4^y = -60$
$p_5 = 40 + 20i$	Wiggle coeff. = 40	$x_{\text{eye}} = y_{\text{eye}} = 20$

slightly modified to improve the aesthetics of the final image. By incorporating these coefficients into complex numbers, we have the equivalent of an elephant contour coded in a set of four complex parameters (see Fig. 1(b)).

The real part of the fifth parameter is the "wiggle parameter," which determines the x -value where the trunk is attached to the body (see the video in Ref. 8). Its imaginary part is used to make the shape more animal-like by fixing the coordinates for the elephant's eye. All the parameters are specified in Table I.

The resulting shape is schematic and cartoonlike but is still recognizable as an elephant. Although the use of the Fourier coordinate expansion is not new,^{2,3} our approach clearly demonstrates its usefulness in reducing the number of parameters needed to describe a two-dimensional contour. In

the special case of fitting an elephant, it is even possible to lower it to four complex parameters and therein implement a well-known saying.

ACKNOWLEDGMENTS

Many thanks to Jean-Yves Tinevez and Marija Žanić, as well as the anonymous reviewers, for revising and improving this article.

¹F. Dyson, "A meeting with Enrico Fermi," *Nature* (London) **427**(6972), 297 (2004).

²F. P. Kuhl and C. R. Giardina, "Elliptic Fourier features of a closed contour," *Comput. Graph. Image Process.* **18**, 236–258 (1982).

³G. Székely, A. Kelemen, C. Brechbühler, and G. Gerig, "Segmentation of 2D and 3D objects from MRI volume data using constrained elastic deformations of flexible Fourier contour and surface models," *Med. Image Anal.* **1**(1), 19–34 (1996).

⁴K. Khairy and J. Howard, "Spherical harmonics-based parametric deconvolution of 3D surface images using bending energy minimization," *Med. Image Anal.* **12**(2), 217–227 (2008).

⁵The interactive Java applet written by Rosemary Kennett, (physics.syr.edu/courses/java/demos/kennett/Epicycle/Epicycle.html).

⁶Interactive Java applet of elliptic descriptors by F. Puente León, (www.vms.ei.tum.de/lehre/vms/fourier/).

⁷J. Wei, "Least square fitting of an elephant," *CHEMTECH* **5**, 128–129 (1975).

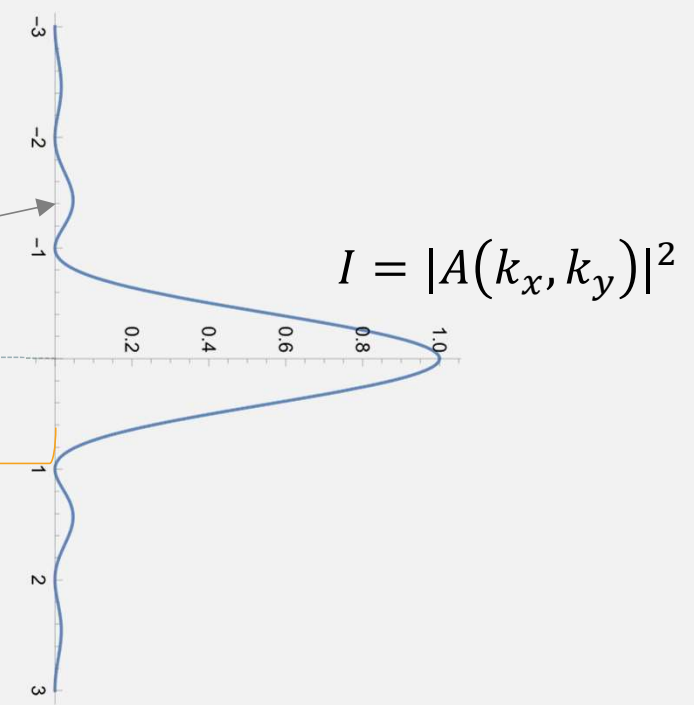
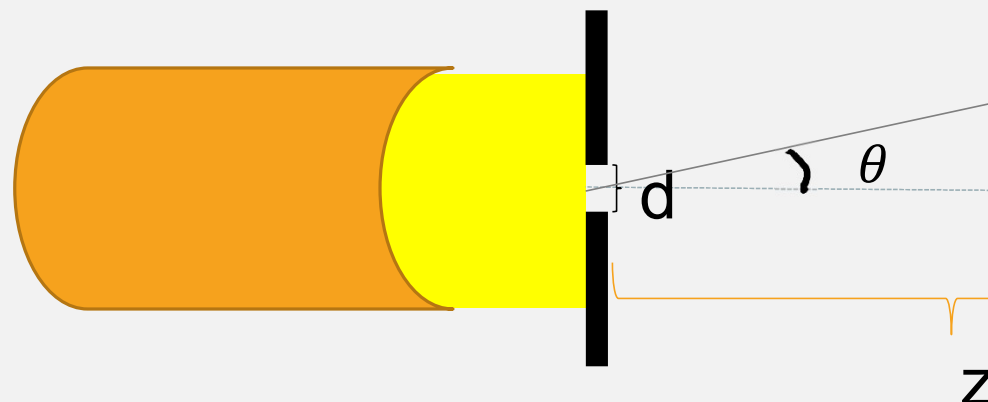
⁸See supplementary material at <http://dx.doi.org/10.1119/1.3254017> for the movie showing the wiggling trunk.

Fraunhofer diffraction

What if we could have a general evolution equation instead of a model?

$$A(k_x, k_y) = \iint_{-\infty - \infty}^{\infty \infty} E_i(x, y) t_M(x, y) e^{-i(k_x x + k_y y)} dx dy$$

$$z \gg d$$



Regge theory – old, but gold

Partial wave expansion: $A^\pm(s, t) = 16\pi \sum_{J=0}^{\infty} (2J + 1) A_J (1 \pm e^{-i\pi J}) P_J(\cos \theta_t)$

with $\cos \theta_t = 1 + \frac{2s}{t - m^2}$ at high energies $P_J(\cos \theta_t) \sim s^J$

The complex J is identified as the Regge trajectory:

$$J = \alpha(t) = \alpha_0 + \alpha' t$$

Regge amplitude:

$$A^\pm(s, t) \sim 16\pi \sum_{l=0}^{\infty} \beta_l^\pm(t) (1 \pm e^{-i\pi\alpha^\pm(t)}) (s/s_0)^{\alpha^\pm(t)}$$

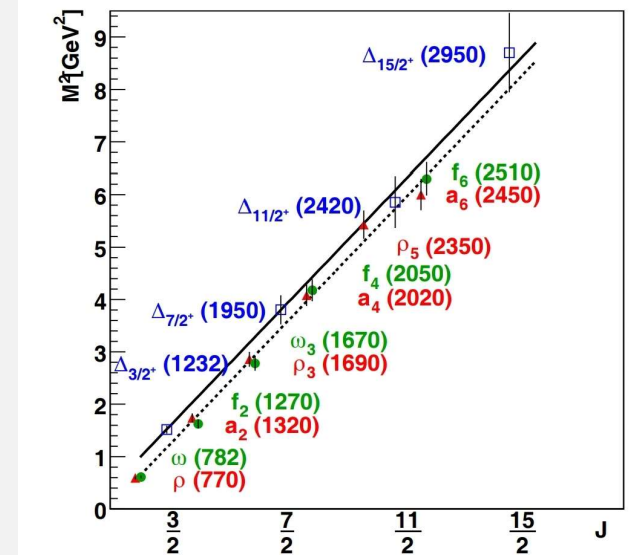


Fig. 1. The leading Regge trajectory: Δ resonances with maximal J in a given mass range. Also shown is the Regge trajectory for mesons with $J = L + S$.

E. Klempt, B. C. Metsch, Eur. Phys. J. A 48, 127 (2012)

Pomeron trajectory = + trajectory with intercept $\alpha_0 = 1 + \varepsilon_0$ greater than one

$$\alpha_P(t) = 1 + \varepsilon_0 + \alpha'_P t$$

Pomeron amplitude $A^+(s, t) = g_a(t)g_b(t)\beta_P(t) \left(i - \cot\left(\frac{\pi\alpha_P(t)}{2}\right) \right) (s/s_0)^{\alpha_P(t)}$

Our initial motivation

A Pomeron-like amplitude is $T(s, t) = g_a(t)g_b(t)\beta_P(t) \left(i - \cot\left(\frac{\pi\alpha_P(t)}{2}\right) \right) e^{[\alpha_P(t)-1]\ln s}$

Fourier transforming it to b-space $\tilde{T}(s, b) = i \int d^2q e^{iq \cdot b} T(s, q^2)$

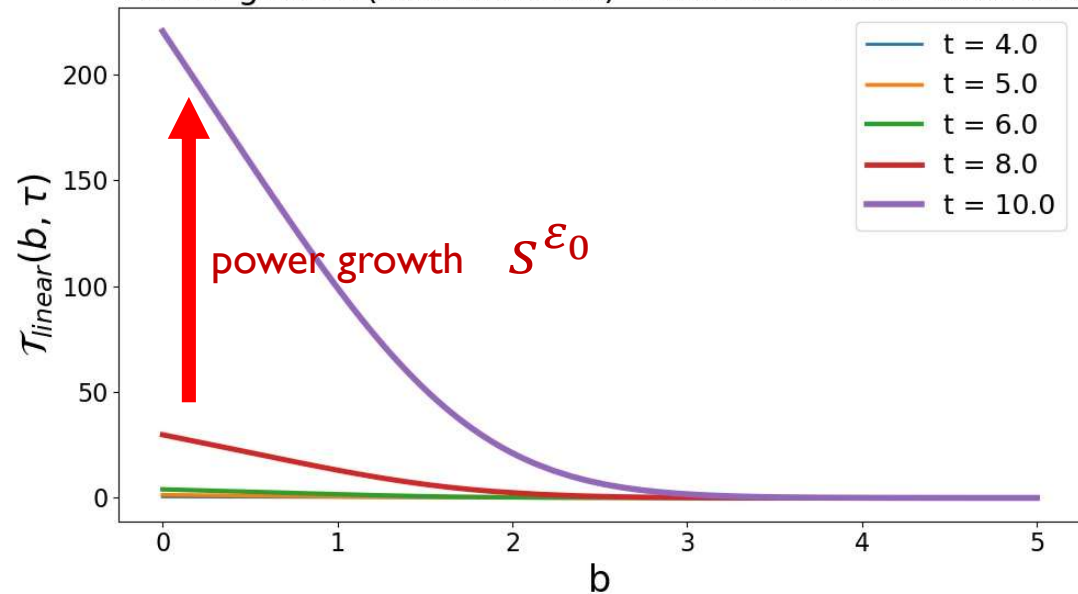
If $g_a(t)$ and $g_b(t)$ do not vary much on t $\tilde{T}(s, b) \sim \tilde{g}_a \tilde{g}_b \tilde{\beta}_P s^{\varepsilon_0} \frac{e^{-\frac{b^2}{4\alpha' \ln s}}}{2\alpha' \ln s}$

We show that $\left(\frac{\partial}{\partial \tau} - \alpha' \nabla_b^2 - \varepsilon_0 \right) \tilde{T}(s, b) = 0$ $\nabla_b^2 = \partial_b^2 + \frac{1}{b} \partial_b$

However:

1. Diffusion alone do not take into account the unitarity saturation
2. Asymptotically the Froissart bound would be violated.
3. We need non-linear terms.

Linear growth (with diffusion) - Gaussian initial condition



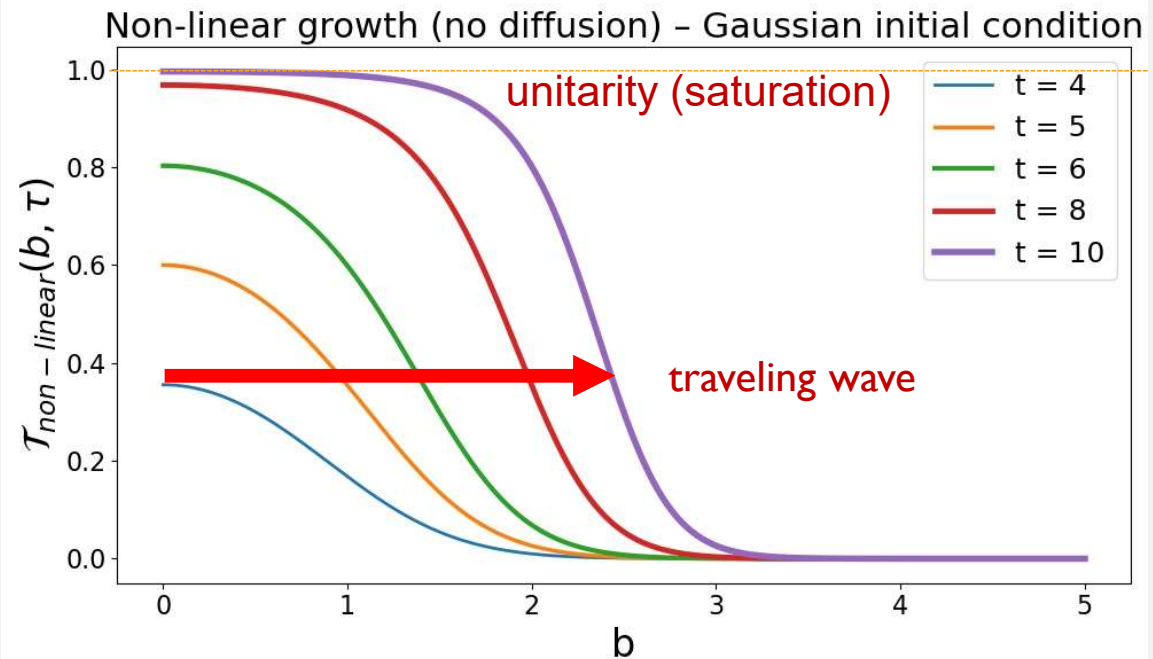
Non-linear correction

$$\left(\frac{\partial}{\partial \tau} - \alpha' \nabla_b^2 - \varepsilon_0 \right) \tilde{T}(s, b) + f(\tilde{T}(s, b)) = 0$$

Linear growth

Violates unitarity and thus Froissart bound

$$\left(\frac{\partial}{\partial \tau} - \alpha' \nabla_b^2 - \varepsilon_0 \right) \tilde{T}(s, b) = 0$$



Regge field theory

Reggeons propagate in two space dimensions \vec{x} and imaginary time τ

The action for a free Pomeron field $A_0 = \int d^2\vec{x} d\tau \mathcal{L}_0(\vec{x}, \tau)$

with the free Lagrangian

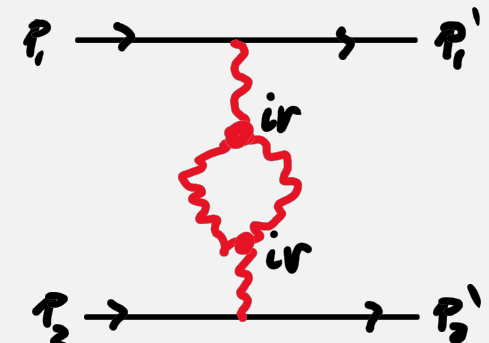
$$\mathcal{L}_0(\vec{x}, \tau) = \frac{1}{2} \varphi^+(\vec{x}, \tau) \overleftrightarrow{\partial} \varphi(\vec{x}, \tau) - \alpha'_0 \nabla \varphi^+(\vec{x}, \tau) \cdot \nabla \varphi(\vec{x}, \tau) - \varepsilon_0 \varphi^+(\vec{x}, \tau) \varphi(\vec{x}, \tau)$$

The interacting part is written in terms of triple Pomeron coupling

$$\mathcal{L}_I = -i\lambda [\varphi^+(\vec{x}, \tau) \varphi^+(\vec{x}, \tau) \varphi(\vec{x}, \tau) + \varphi^+(\vec{x}, \tau) \varphi(\vec{x}, \tau) \varphi(\vec{x}, \tau)]$$

H. D. Abarbanel, J. D. Bronzan, R. L. Sugar, and A. R. White, Physics Reports 21, 119 (1975)

In RFT the imaginary time τ is the rapidity $\tau = \ln(s)$



Typical graph contributing to the amplitude

We flipped the sign of the interaction term

$$\mathcal{L}_I = +i\lambda [\varphi^+(\vec{x}, \tau) \varphi^+(\vec{x}, \tau) \varphi(\vec{x}, \tau) + \varphi^+(\vec{x}, \tau) \varphi(\vec{x}, \tau) \varphi(\vec{x}, \tau)]$$

To avoid the imaginary term one can transform the Gribov fields such as $q = i\varphi^+$ and $p = i\varphi^-$

$$\mathcal{L} = \frac{1}{2} q \partial_\tau p + \alpha' \nabla_b q \cdot \nabla_b p - \varepsilon_0 q p - \lambda q(p+q)p$$

The Hamiltonian is given

$$H = \int d^2 b \{ -\alpha' \nabla_b q(b) \cdot \nabla_b p(b) + \varepsilon_0 q(b)p(b) + \lambda q(b)[p(b) + q(b)]p(b) \}$$

Where q and p are creation and annihilation operators respectively satisfying the commutation relation

$$[p(b, \tau), q(b', \tau)] = -\delta^{(2)}(b - b')$$

In discretized two-dimensional b -space lattice it was shown that for $\varepsilon_0 > 0$ the zero-energy ground state $|\phi_0\rangle$ acquires a non-zero energy state $|\phi_1\rangle$ which approaches a coherent state

$$|\phi_1\rangle = e^{-\frac{\varepsilon_0}{\lambda} \int q(b, 0) db} |\phi_0\rangle \quad \text{such that} \quad p(b, 0)|\phi_1\rangle = \frac{\varepsilon_0}{\lambda} |\phi_1\rangle$$

A generalized state is written as

V. Alessandrini, D. Amati, and M. Ciafaloni, Nucl. Phys. B 130, 429 (1977)

$$|\psi(\tau)\rangle = e^{-\hat{M}(\tau)} |\phi_0\rangle$$

n+1 correlation functions

With the operator

$$\hat{M}(\tau) = \sum_{n=1}^{\infty} \frac{1}{n!} \int d^2 \bar{b}_1 \dots d^2 \bar{b}_n q(\bar{b}_1) \dots q(\bar{b}_n) G_n(\tau, \bar{b}_1, \dots, \bar{b}_n)$$


Expanding $|\psi\rangle = e^{-\widehat{M}(\tau)}|\phi_0\rangle = (1 - \widehat{M} + \frac{1}{2!}\widehat{M}^2 + \dots)|\phi_0\rangle$

$$= \left\{ 1 - \left(\int_b \hat{q}(\vec{b}) G_1(\vec{b}; \tau) + \frac{1}{2!} \int_{b_1, b_2} \hat{q}(\vec{b}_1) \hat{q}(\vec{b}_2) G_2(\vec{b}_1, \vec{b}_2; \tau) + \dots \right) + \frac{1}{2!} \left(\int_b \hat{q}(\vec{b}) G_1(\vec{b}; \tau) + \frac{1}{2!} \int_{b_1, b_2} \hat{q}(\vec{b}_1) \hat{q}(\vec{b}_2) G_2(\vec{b}_1, \vec{b}_2; \tau) + \dots \right)^2 + \right. \\ \left. - \frac{1}{3!} \left(\int_b \hat{q}(\vec{b}) G_1(\vec{b}; \tau) + \frac{1}{2!} \int_{b_1, b_2} \hat{q}(\vec{b}_1) \hat{q}(\vec{b}_2) G_2(\vec{b}_1, \vec{b}_2; \tau) + \dots \right)^3 + \dots \right\} |\phi_0\rangle$$

Collecting powers of q such as $\int_b \hat{q}(\vec{b}), \int_{b_1, b_2} \hat{q}(\vec{b}_1) \hat{q}(\vec{b}_2), \dots$ solving the Schrodinger equation

We obtain $\partial_\tau G_1(b, \tau) = (\varepsilon_0 + \alpha' \nabla_b^2) G_1(b, \tau) + \lambda G_1^2(b, \tau) - \lambda G_2(b, b, \tau)$

$$\begin{aligned} \partial_\tau G_2(b, b', \tau) &= (\varepsilon_0 + \alpha' \nabla_b^2) G_2(b, b', \tau) + (\varepsilon_0 + \alpha' \nabla_{b'}^2) G_2(b, b', \tau) - 2\lambda \delta^2(b - b') G_1(b, \tau) \\ &\quad + 4\lambda [G_1(b, \tau)] G_2(b, b', \tau) - 2\lambda G_3(b, b, b', \tau) \end{aligned}$$

.

.

In the semiclassical approximation $\partial_\tau G_1(b, \tau) = (\varepsilon_0 + \alpha' \nabla_b^2) G_1(b, \tau) + \lambda G_1^2(b, \tau)$

Our assumption

$$G_1(b, \tau) \propto i\tilde{T}(b, \tau)$$

2-POINT CORRELATION FUNCTION \propto ELASTIC SCATTERING AMPLITUDE

We are focused in the complex equation $T(s, t) = T_R(s, t) + iT_I(s, t)$

In b-space $\tilde{T}(s, \vec{b}) = \int d^2 \vec{q} e^{-i\vec{b} \cdot \vec{q}} T(s, -q^2)$

$$\partial_\tau (i\tilde{T}(b, \tau)) = (\varepsilon_0 + \alpha' \nabla_b^2) (i\tilde{T}(b, \tau)) + \lambda (i\tilde{T}_I(b, \tau))^2$$

H. Kakkad, A. K. K. and P. Kotko, Eur. Phys. J. C 82 (2022) 9, 830

The imaginary and real parts respectively are

$$\frac{\partial \tilde{T}_I}{\partial \tau} = (\alpha' \nabla_b^2 + \varepsilon_0) \tilde{T}_I - \lambda \tilde{T}_I^2 + \lambda \tilde{T}_R^2$$

Interesting analogy

$$\tilde{T}_I(\tau, b) \Leftrightarrow N(\tau, k)$$

$$\frac{\partial \tilde{T}_R}{\partial \tau} = (\alpha' \nabla_b^2 + \varepsilon_0) \tilde{T}_R - 2\lambda \tilde{T}_R \tilde{T}_I$$

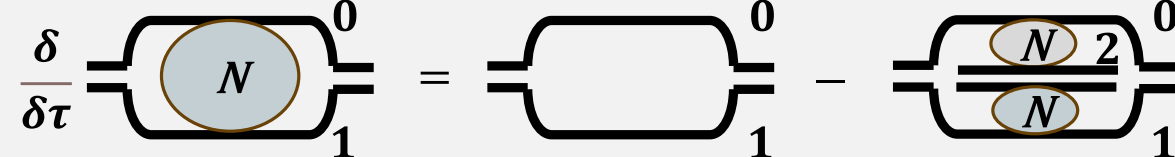
$$\tilde{T}_R(\tau, b) \Leftrightarrow O(\tau, k)$$

They look like BK type equations: $\frac{\partial N}{\partial \tau} = \bar{\alpha} \chi(-\partial_L) N - \bar{\alpha} N^2 ; \quad N(\tau, k) = N \left(\frac{k^2}{Q_s^2(\tau)} \right)$

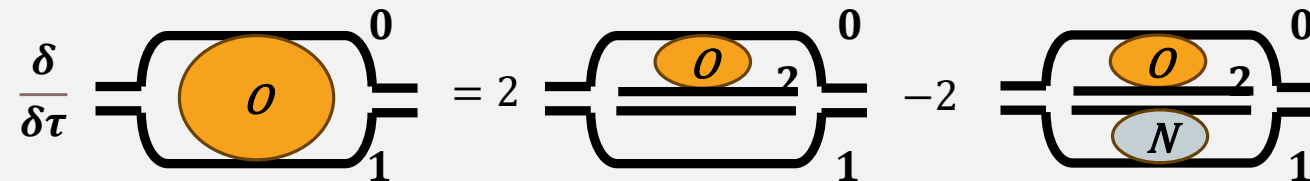
S. Munier and R. B. Peschanski, Phys. Rev. Lett. 91, 232001 (2003)

dipole picture

Pomeron



oddron



Y. V. Kovchegov, L. Szymanowski, and S. Wallon, Phys. Lett. B 586, 267 (2004)

Our first results

As initial conditions at $s_{fix} = 500 \text{ GeV}^2$: two different models in b-space: KFK and BSW

$$\tilde{T}_R(s_{fix}, b) = \tilde{T}_R^{KFK}(s_{fix}, b)$$

$$\tilde{T}_I(s_{fix}, b) = \tilde{T}_I^{KFK}(s_{fix}, b)$$

A. K. K., E. Ferreira, and T. Kodama, Eur. Phys. J. C 74, 3175 (2014)

$$\tilde{T}_R(s_{fix}, b) = \tilde{T}_R^{BSW}(s_{fix}, b)$$

$$\tilde{T}_I(s_{fix}, b) = \tilde{T}_I^{BSW}(s_{fix}, b)$$

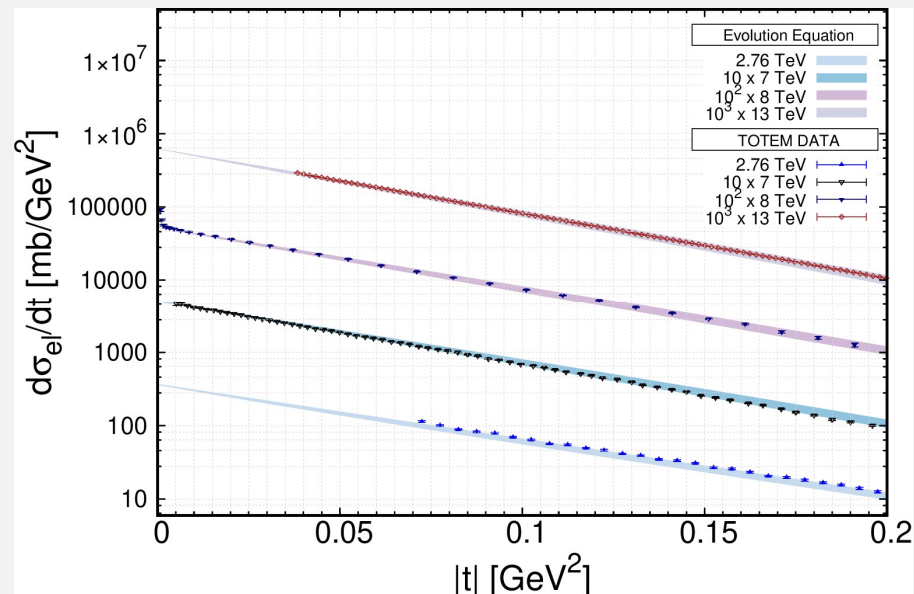
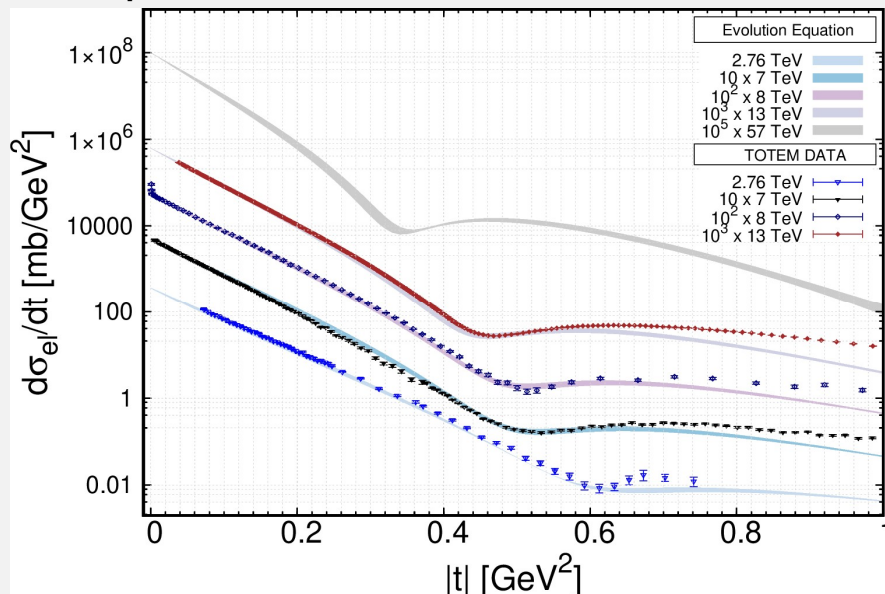
C. Bourrely, J. Soffer, and T. T. Wu, Phys. Rev. D 19, 3249 (1979)

Boundary conditions set $\tilde{T}_I(s, b \rightarrow \infty) = \tilde{T}_R(s, b \rightarrow \infty) = 0$

The obtained parameters are

	$\alpha' (\text{GeV}^{-2})$	ε_0	λ/ε_0
KFK	0.105	0.129	0.712
BSW	0.090	0.140	0.820

Our predictions for differential cross section



The integrated quantities are

	\sqrt{s} [TeV]	σ_{tot} [mb]	ρ	B [GeV $^{-2}$]
KFK initial condition	2.76	84.31	0.123	17.28
	7	99.07	0.117	18.47
	8	101.32	0.116	18.65
	13	109.78	0.113	19.32
	57	138.32	0.105	21.55
BSW initial condition	2.76	83.14	0.143	19.69
	7	98.40	0.134	21.12
	8	100.73	0.132	21.34
	13	109.52	0.127	22.15
	57	142.30	0.115	24.87
TOTEM	2.76	84.7 ± 3.3	–	17.1 ± 0.30
	7	98.0 ± 2.5	0.145 ± 0.091	19.73 ± 0.40
	8	101.7 ± 2.9	0.12 ± 0.03	19.74 ± 0.28
	13	110.6 ± 3.4	0.10 ± 0.01	20.40 ± 0.01
ATLAS	7	95.35 ± 0.38	0.14 (fix)	19.73 ± 0.14
	8	96.07 ± 0.18	0.136 (fix)	19.74 ± 0.05
AUGER	57	133 ± 29	–	–

G. Antchev et al.(TOTEM Collaboration), Eur. Phys.J.C 80, 91(2020); EPL 101, 21002(2013); Eur. Phys.J.C 76, 661(2016); Eur. Phys.J.C 79, 103(2019)

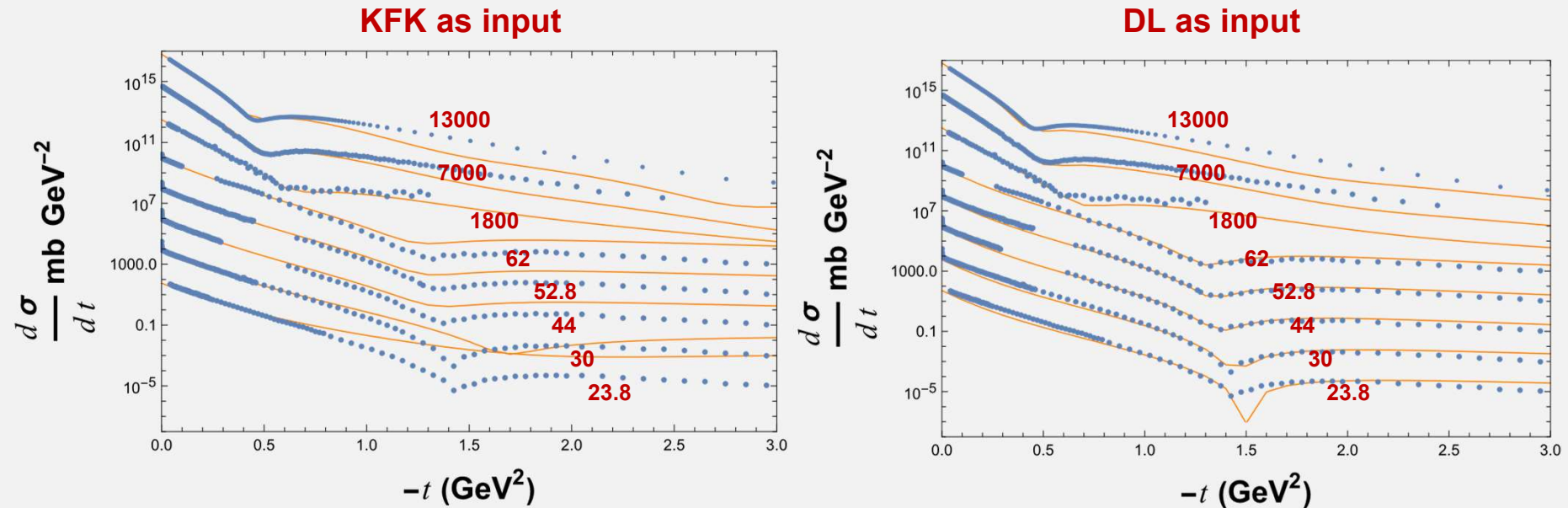
G. Aad et al.(ATLAS Collaboration), Nucl. Phys.B 889, 486(2014); Phys. Lett. B 761, 158 (2016)

P. Abreu et al. (Pierre Auger Collaboration) Phys. Rev. Lett. 109, 062002 (2012)

Could it be like a broken clock?

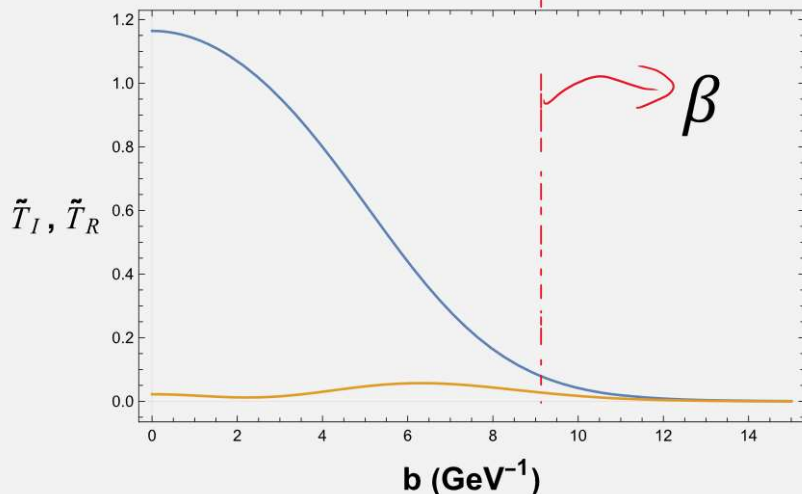


Some problems at ISR energies

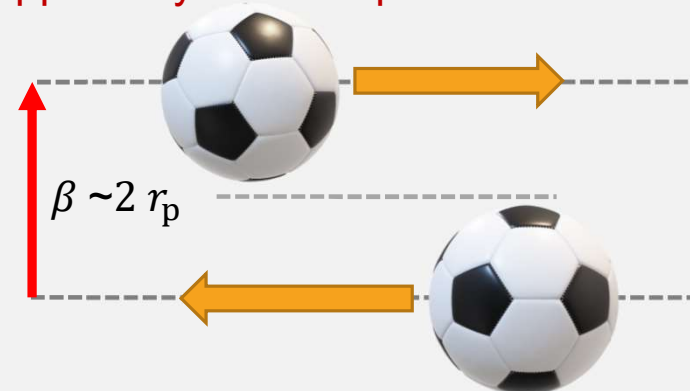


Turning off diffusion (phenomenologically)

$$\frac{\partial \tilde{T}}{\partial \tau} = \alpha' \theta(b - \beta) \nabla_b^2 \tilde{T} + \varepsilon_0 \tilde{T} \left(1 - \frac{\lambda}{\varepsilon_0} \tilde{T} \right) \quad \text{with} \quad \nabla_b^2 = \partial_b^2 + \frac{1}{b} \partial_b$$



Apparently the data prefers to shrink diffusion range ...



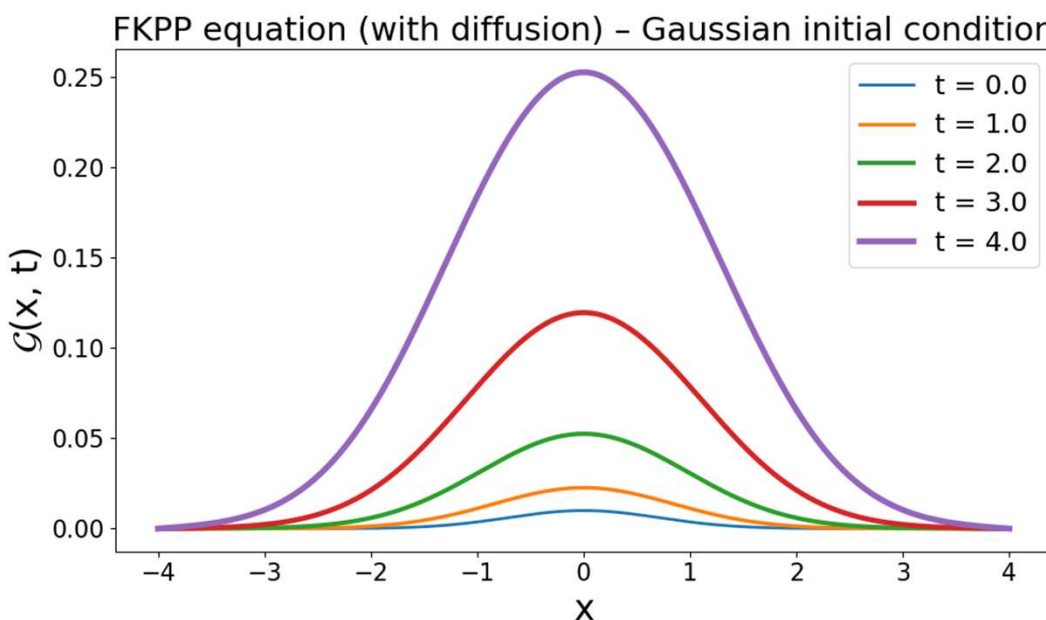
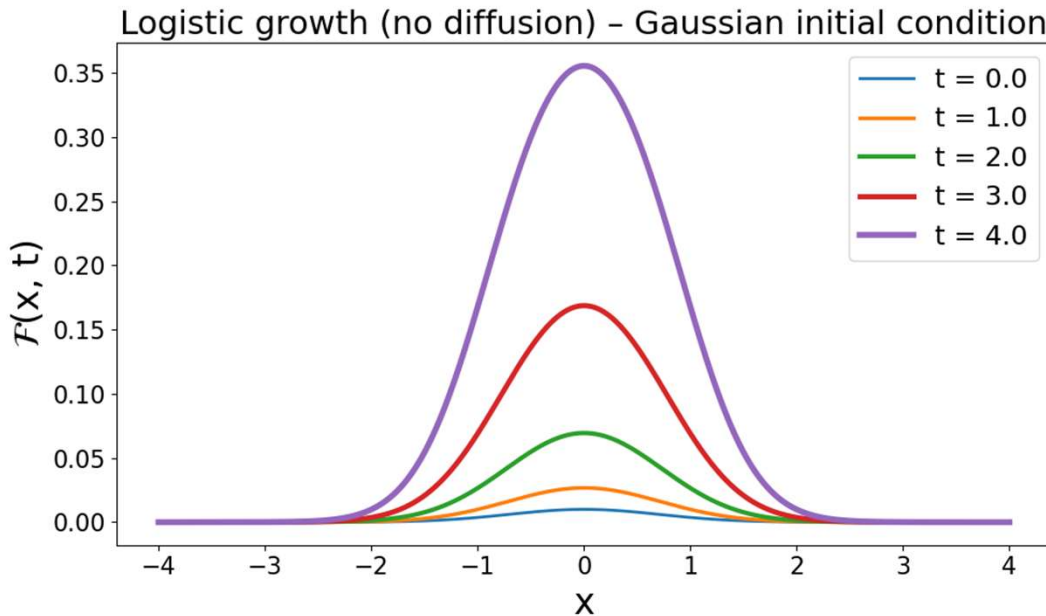
Assuming $\alpha' \rightarrow 0$ we have just a **complex differential logistic equation**

$$\frac{\partial \tilde{T}}{\partial \tau} = \varepsilon_0 \tilde{T} \left(1 - \frac{\lambda}{\varepsilon_0} \tilde{T} \right)$$

With an analytic solution $\tilde{T}(\tau, b) = \frac{\tilde{T}_0(\tau_0, b)}{\left(1 + i \frac{\lambda}{\varepsilon_0} \tilde{T}_0(\tau_0, b) \right) e^{-\varepsilon_0(\tau-\tau_0)} - i \frac{\lambda}{\varepsilon_0} \tilde{T}_0(\tau_0, b)}$

Where $\tilde{T}_0(\tau_0, b)$ is the initial condition -- models in b space

Why can we turn off diffusion?



$$\frac{\partial F(x, t)}{\partial t} = \varepsilon_0 F(x, t) \left(1 - \frac{\lambda}{\varepsilon_0} F(x, t) \right)$$

$$F_0(x) = F(x, t_0) = A e^{-x^2/\beta} \quad \text{I.C.}$$

Analytic solution is given

$$F(t, x) = \frac{F_0(x) e^{\varepsilon_0 \tau}}{1 + \frac{\lambda}{\varepsilon_0} F_0(x) (e^{\varepsilon_0 \tau} - 1)}$$

$$\frac{\partial G(x, t)}{\partial t} = D \frac{\partial^2 G(x, t)}{\partial x^2} + \varepsilon_0 G(x, t) \left(1 - \frac{\lambda}{\varepsilon_0} G(x, t) \right)$$

$$G_0(x) = G(x, t_0) = A e^{-x^2/\beta} \quad \text{I.C.}$$

Numeric solution...

Complex logistic equation \Leftrightarrow Linear relaxation equation

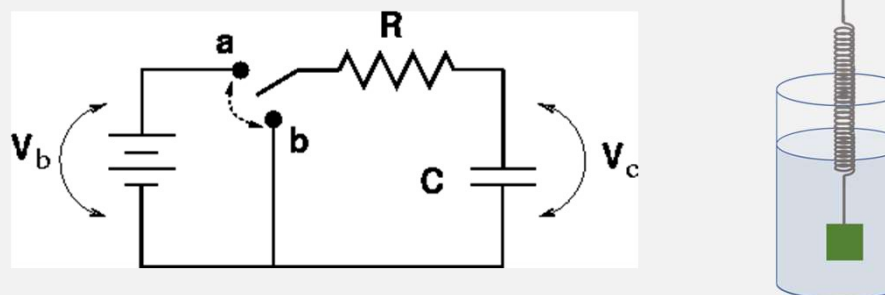
Changing the function $u(\tau, b) = \frac{1}{\tilde{T}(\tau, b)}$ we obtain $\left(\frac{\partial}{\partial \tau} + \varepsilon_0 \right) u(\tau, b) = -i \lambda$

With the solution $u(\tau, b) = A(b)e^{-\varepsilon_0 \tau} - i \frac{\lambda}{\varepsilon_0}$ $\Rightarrow \tilde{T}(\tau, b) = \frac{1}{A(b)e^{-\varepsilon_0 \tau} - i \frac{\lambda}{\varepsilon_0}}$

Where $A(b)$ plays the role of an integration constant for τ . Using $\tilde{T}(\tau_0, b) = \tilde{T}_0(\tau_0, b)$

we obtain $A(b)$ and then $\tilde{T}(\tau, b) = \frac{\tilde{T}_0(\tau_0, b)}{\left(1 + i \frac{\lambda}{\varepsilon_0} \tilde{T}_0(\tau_0, b) \right) e^{-\varepsilon_0(\tau-\tau_0)} - i \frac{\lambda}{\varepsilon_0} \tilde{T}_0(\tau_0, b)}$

This invites an analogy with damped classical systems, such as RC circuits or overdamped harmonic oscillators, where damping plays the role of a mechanism that conducts the system toward equilibrium (unitarity/saturation).



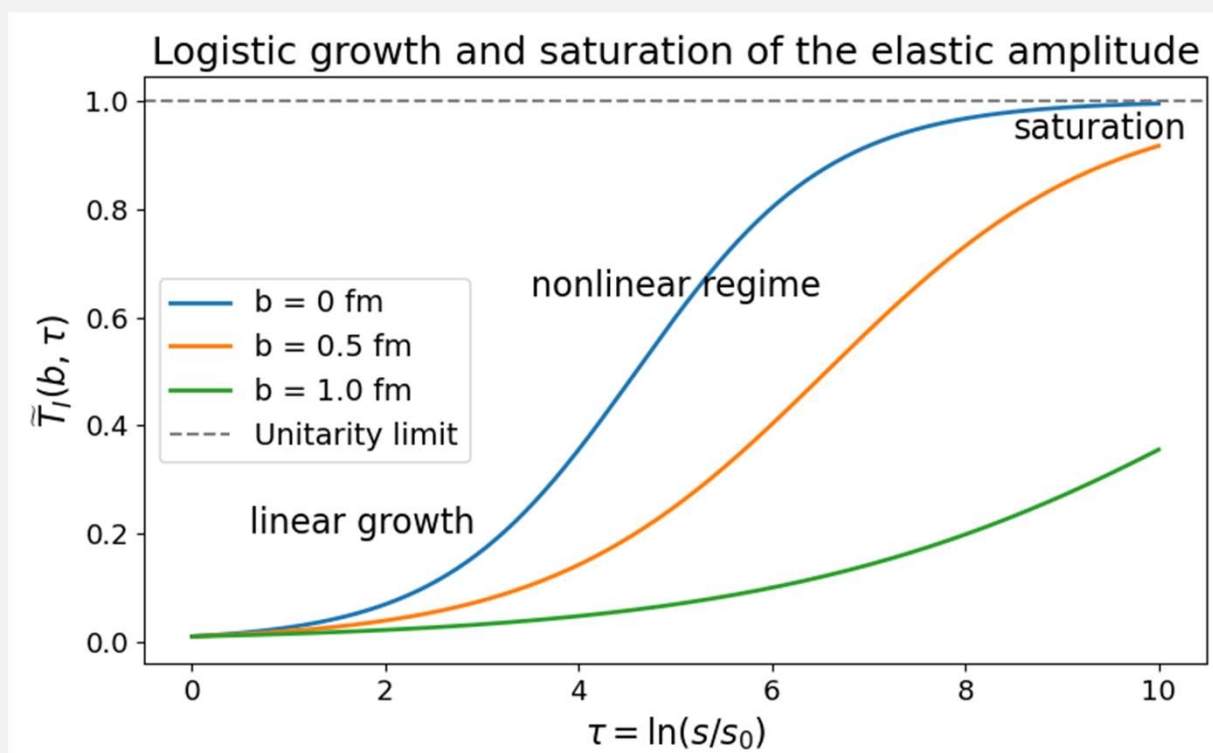
The logistic behaviour

The real and imaginary parts of the evolution equation are

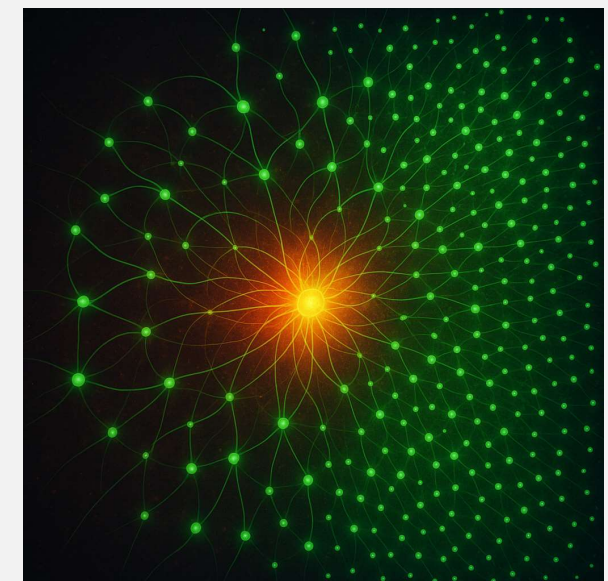
$$\frac{\partial \tilde{T}_I}{\partial \tau} = \varepsilon_0 \left[\tilde{T}_I \left(1 - \frac{\lambda}{\varepsilon_0} \tilde{T}_I \right) + \frac{\lambda}{\varepsilon_0} \tilde{T}_R^2 \right]$$

$$\frac{\partial \tilde{T}_R}{\partial \tau} = \varepsilon_0 \tilde{T}_R \left(1 - 2 \frac{\lambda}{\varepsilon_0} \tilde{T}_I \right)$$

Neglecting $\tilde{T}_R^2 \rightarrow 0$ the imaginary part is simply logistic



$$\frac{\partial \tilde{T}_I}{\partial \tau} = \varepsilon_0 \left[\tilde{T}_I \left(1 - \frac{\lambda}{\varepsilon_0} \tilde{T}_I \right) \right]$$



$\tau = \ln s$

From our effective Lagrangian

$$\mathcal{L}'(\vec{x}, \tau) = \frac{1}{2} \varphi^+(\vec{x}, \tau) \overleftrightarrow{\partial_\tau} \varphi(\vec{x}, \tau) - \varepsilon_0 \varphi^+(\vec{x}, \tau) \varphi(\vec{x}, \tau) + i\lambda [\varphi^+(\vec{x}, \tau) \varphi^+(\vec{x}, \tau) \varphi(\vec{x}, \tau) + \varphi^+(\vec{x}, \tau) \varphi(\vec{x}, \tau) \varphi(\vec{x}, \tau)]$$

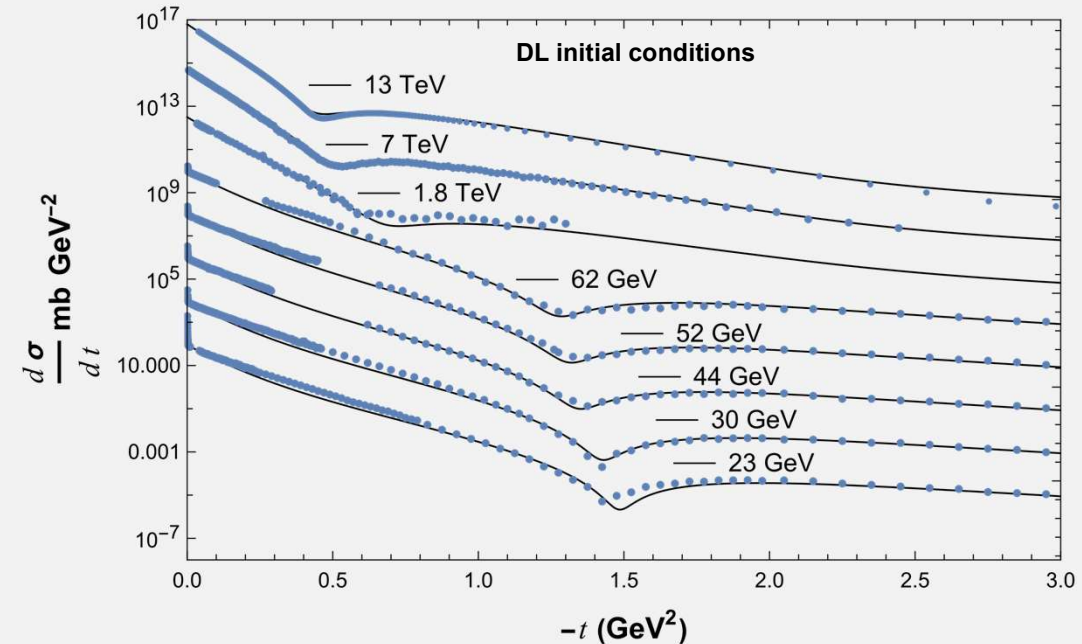
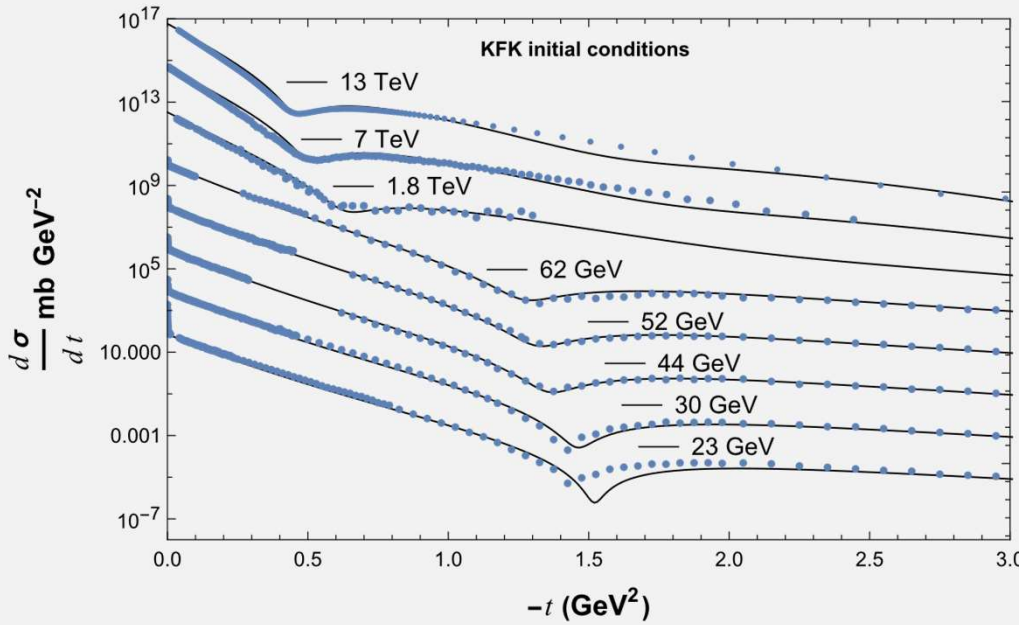
We derive

$$\tilde{T}(\tau, b) = \frac{\tilde{T}_0(\tau_0, b)}{\left(1 + i \frac{\lambda}{\varepsilon_0} \tilde{T}_0(\tau_0, b)\right) e^{-\varepsilon_0(\tau-\tau_0)} - i \frac{\lambda}{\varepsilon_0} \tilde{T}_0(\tau_0, b)}$$

It is subjected to high energy and mathematical theorems

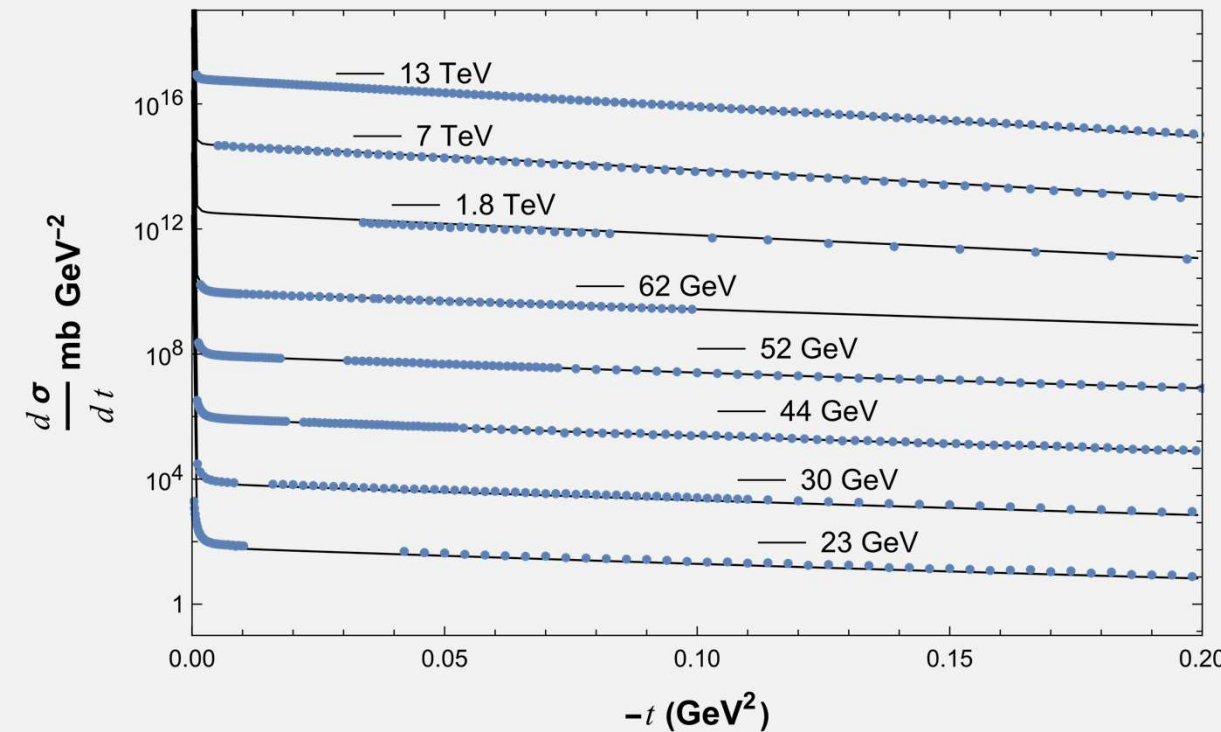
1. It is satisfies unitarity ✓
2. For every physically resonable profiles it satisfies Froissart-Martin limit ✓
3. We rigourously prove that it admits unique solution for each initial condition ✓
4. We prove that our complex solution is holomorphic and it obeys the dispersion relations ✓

Some results for different initial conditions



I.C.	ε_0	λ
KFK	0.122	0.088
DL	0.128	0.103
BSW	0.124	0.092
Real BB	0.135	0.095

In the very forward region



Using our previous model for the forward as I.C

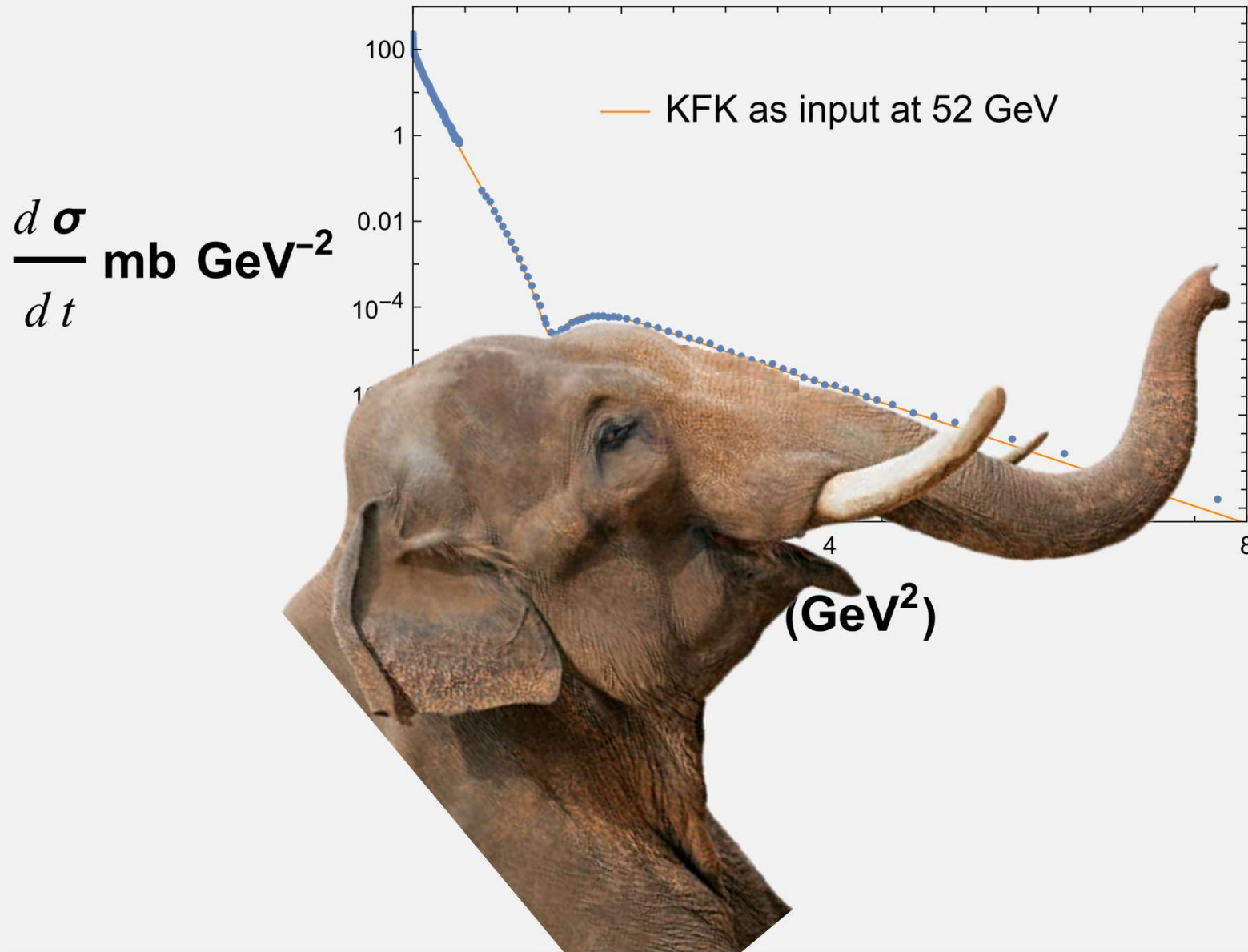
A.K.K., J.Phys.G 46 (2019) 12, 125001

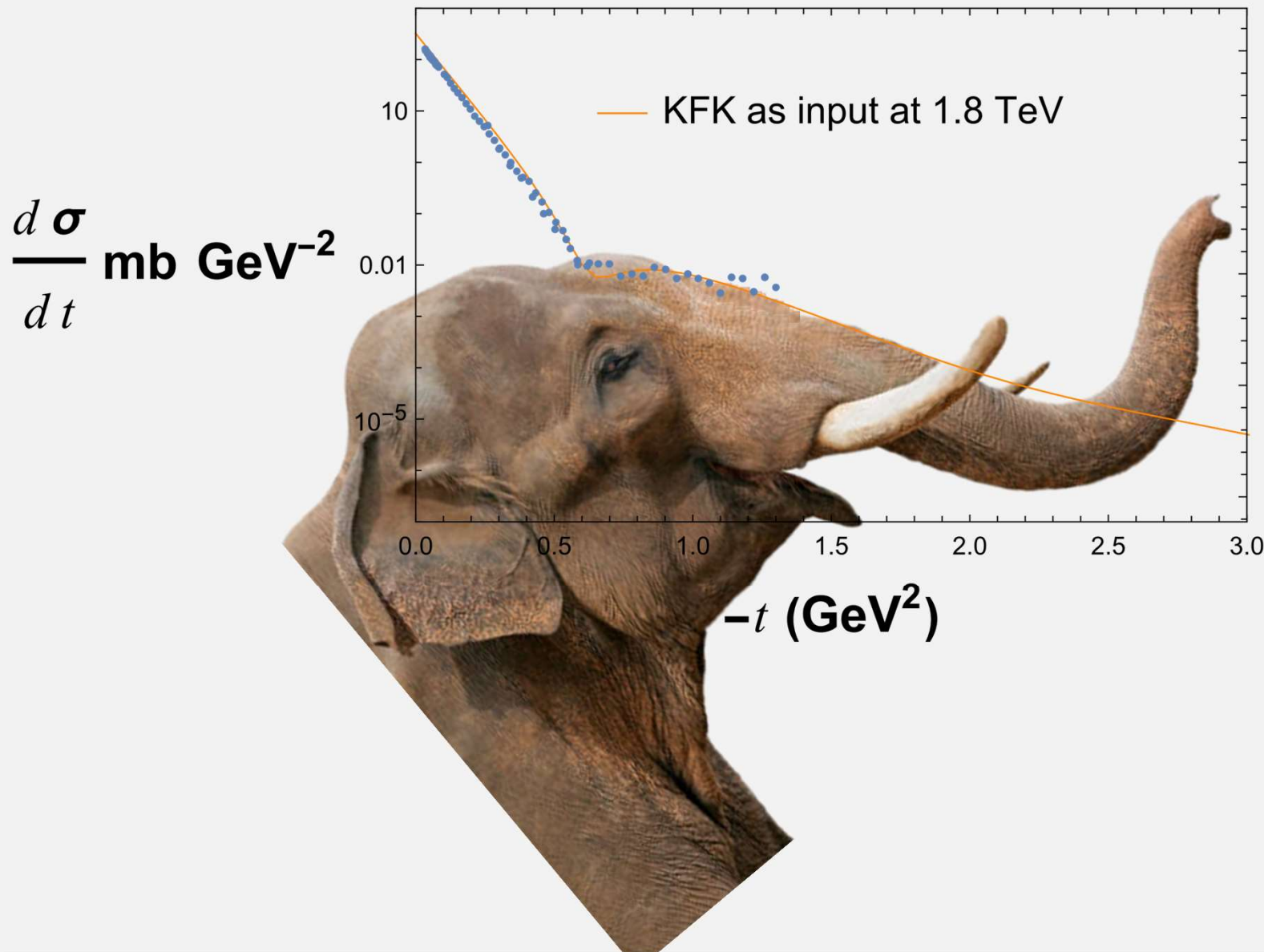
I.C.	ε_0	λ
AKK-forward	0.15	0.15

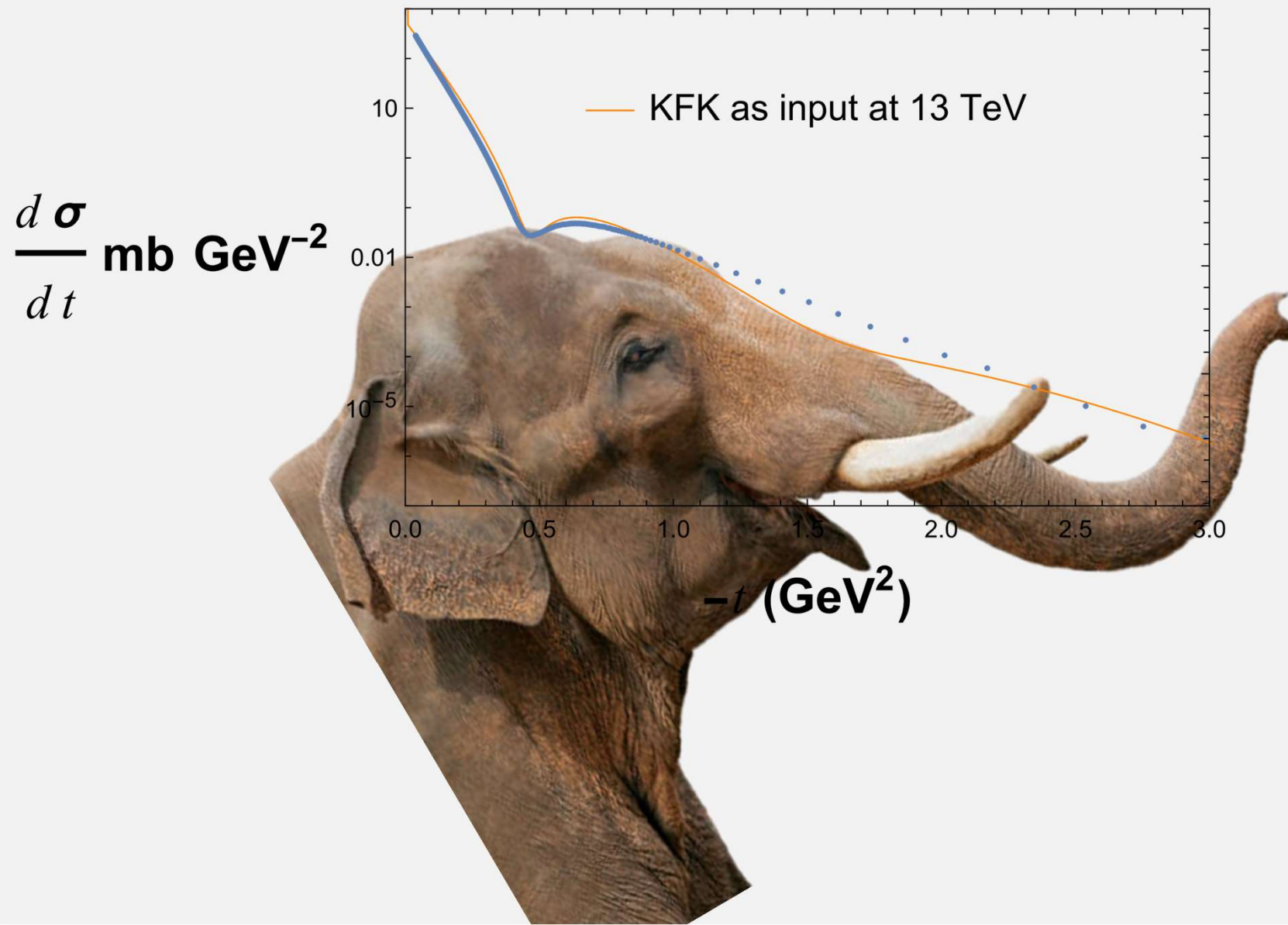
Interestingly $\frac{\lambda}{\varepsilon_0} \rightarrow 1$

end the equation simplifies

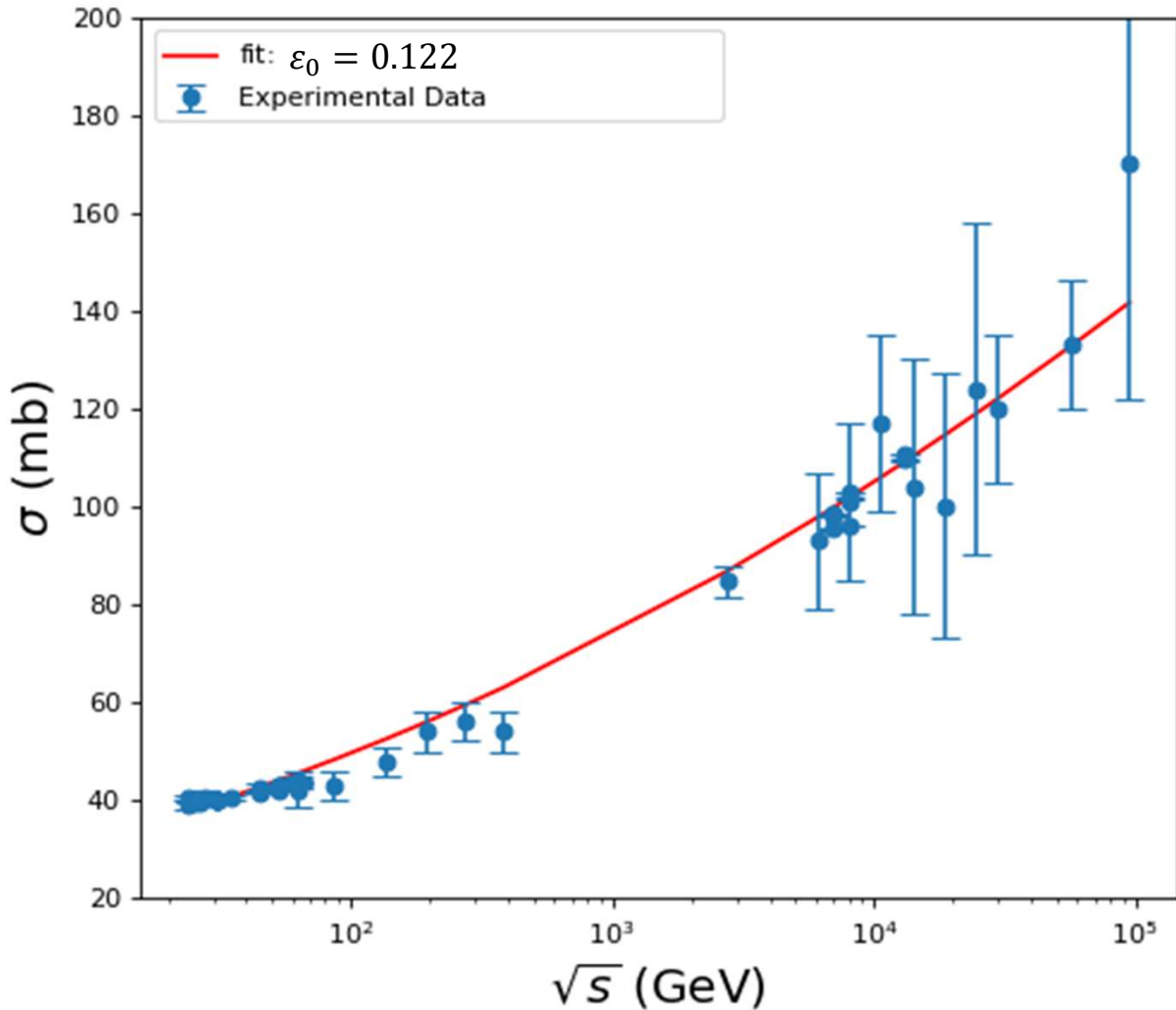
$$\frac{\partial \tilde{T}}{\partial \tau} = \varepsilon_0 \tilde{T} \left(1 - \frac{\lambda}{\varepsilon_0} \tilde{T} \right) \rightarrow \frac{\partial \tilde{T}}{\partial \tau} = \varepsilon_0 \tilde{T} (1 - \tilde{T})$$







The total cross section



A single parameter ε_0

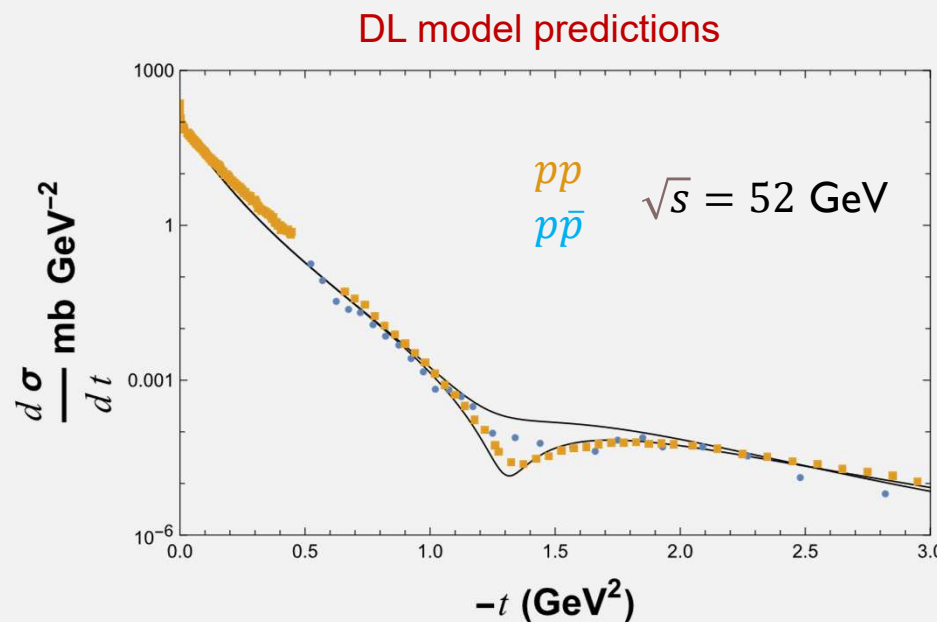
Dip difference in crossed channel (Odderon)?

Odderon: an odd exchange in elastic scattering (changes sign for pp and $p\bar{p}$)

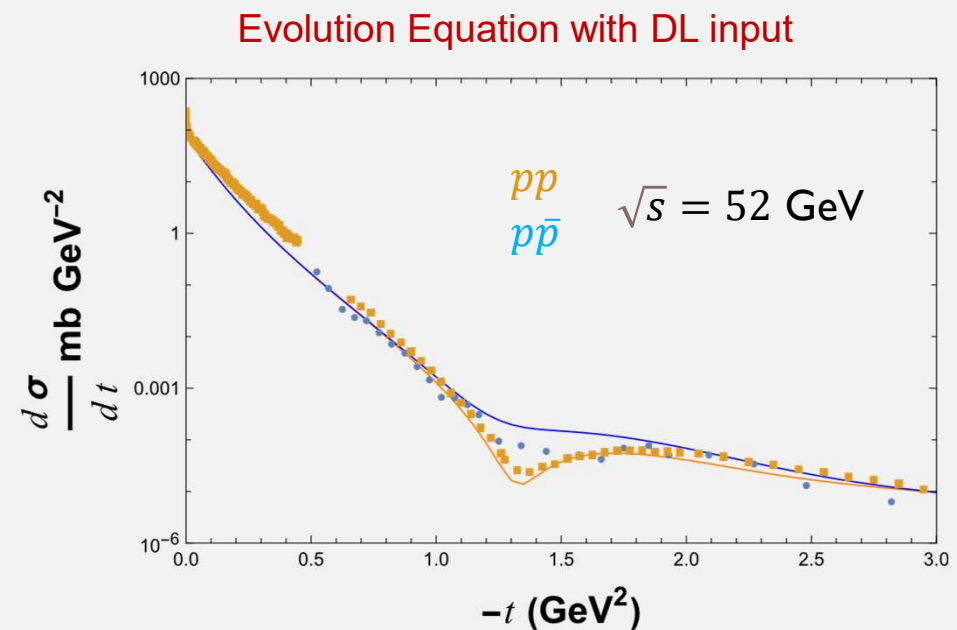
L. Lukaszuk, B. Nicolescu, Lett. Nuovo Cim. 8, 405 (1973)

Few energies to directly compare pp with $p\bar{p}$

*A. Breakstone et al, Phys. Rev. Lett. 54, 2180 (1985)
U. Amaldi et al, Nucl.Phys.B 166 (1980) 301-320, (1980)*



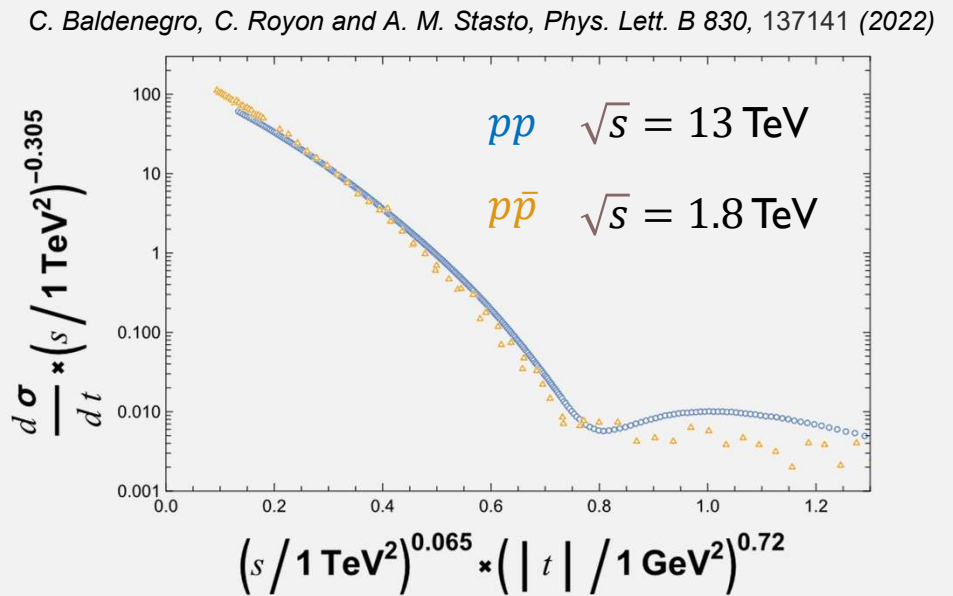
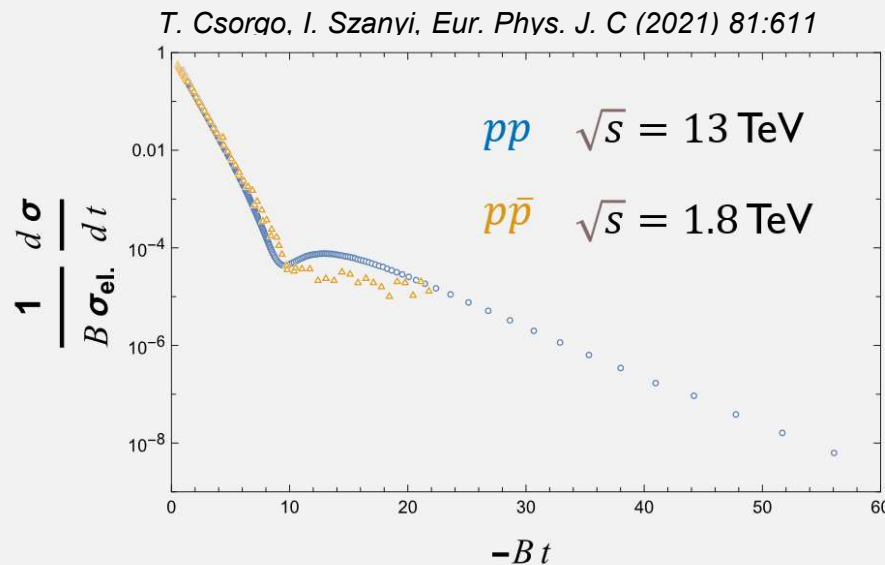
The dip difference due to the tri-gluon exchange



Same evolution equation, but different I.C.

Dip difference in crossed channel (odderon)?

Scaling at TeV energies



Comparing the shape of the differential cross section between crossed channel...

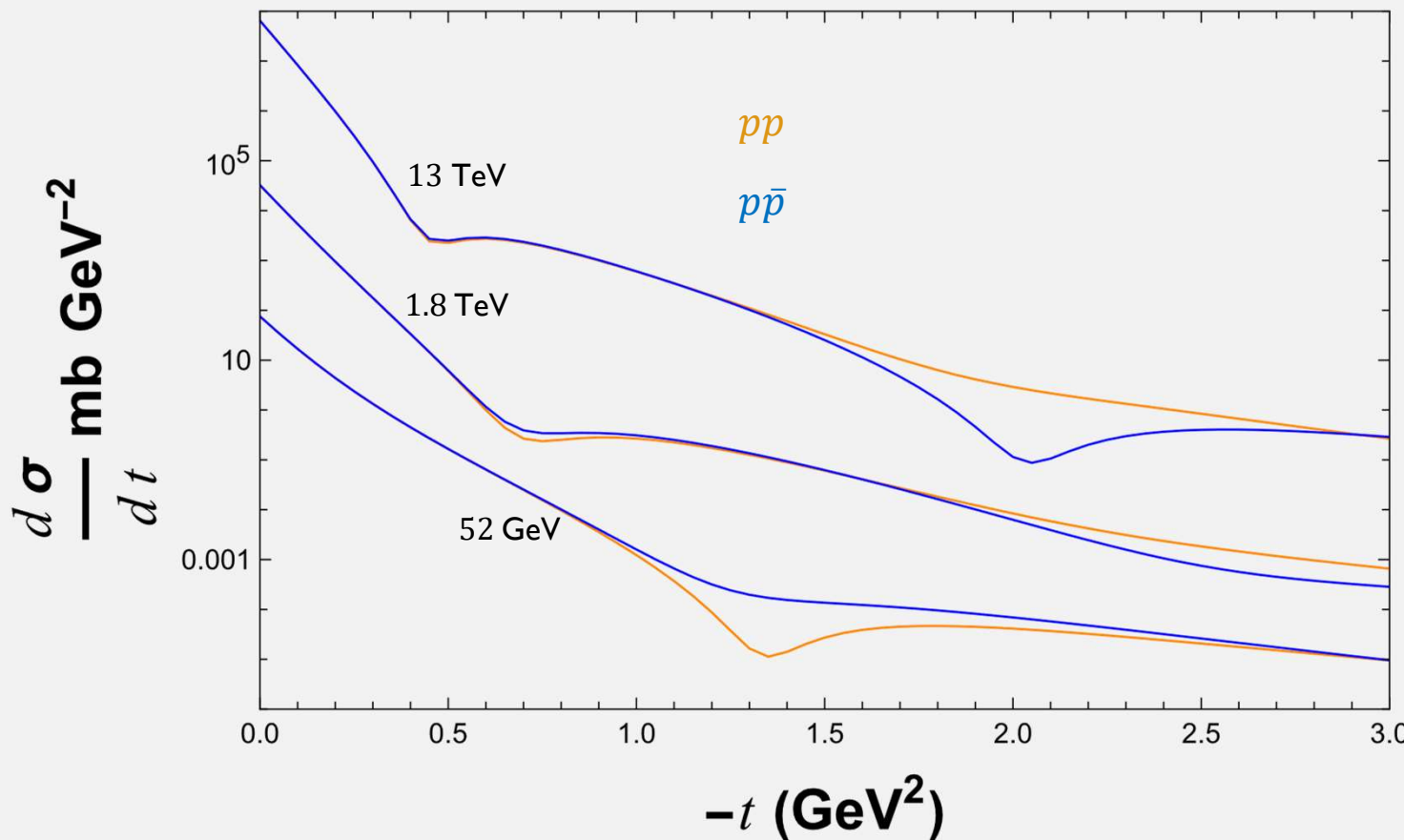
V. M. Abazov et al. (D0 and TOTEM Collaboration) Phys. Rev. Lett. 127, 062003 (2021)

Does the dip-bump difference indicates the existence of the odderon?

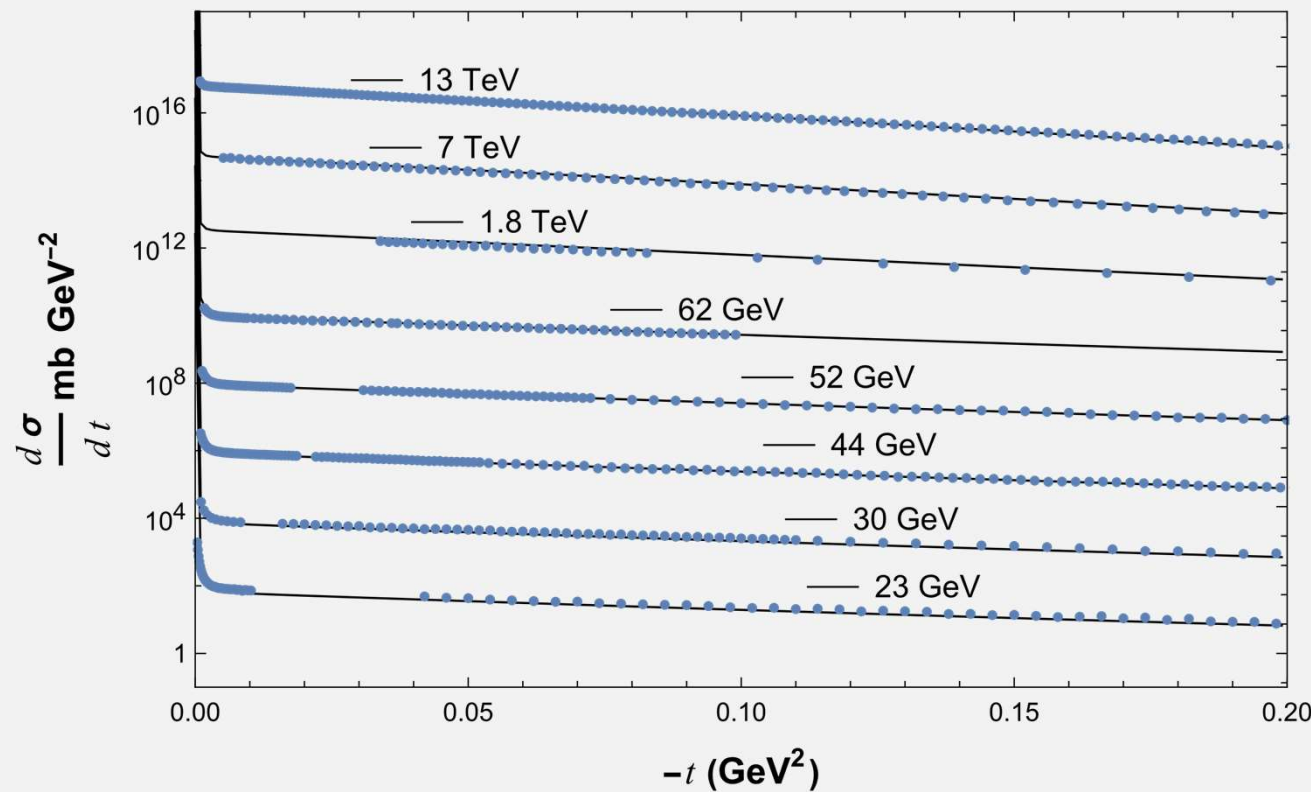
Dip evolution for different initial conditions

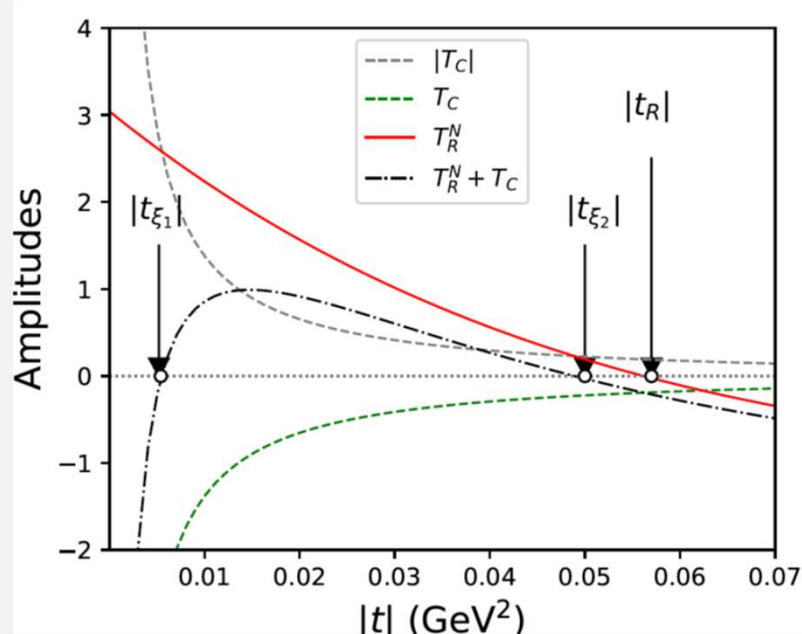
Note that at high energies the “first” dip structure for pp and $p\bar{p}$ seems to converge!

Evolution Equation with DL input



The real-Coulomb interference (very forward scattering)





For pp the Coulomb amplitude is negative

The real nuclear amplitude is positive in the forward range (Martin's theorem)

A. Martin, Phys. Lett. B 404, 137 (1997).

Let $T_R(s, t)$ be the real part of the sum of the nuclear and Coulomb pp amplitudes,

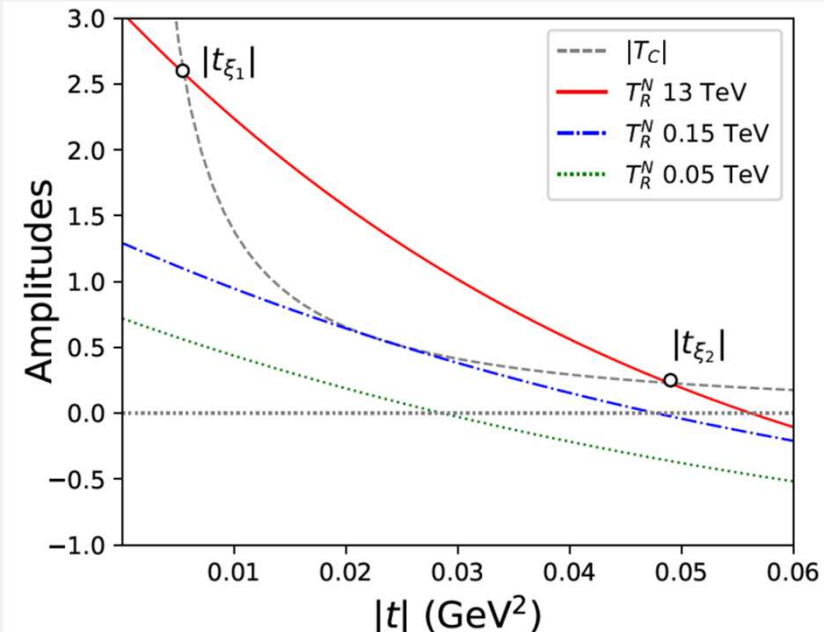
$$T_R(s, t) \equiv T_R^N(s, t) + T_C(s), \quad (8)$$

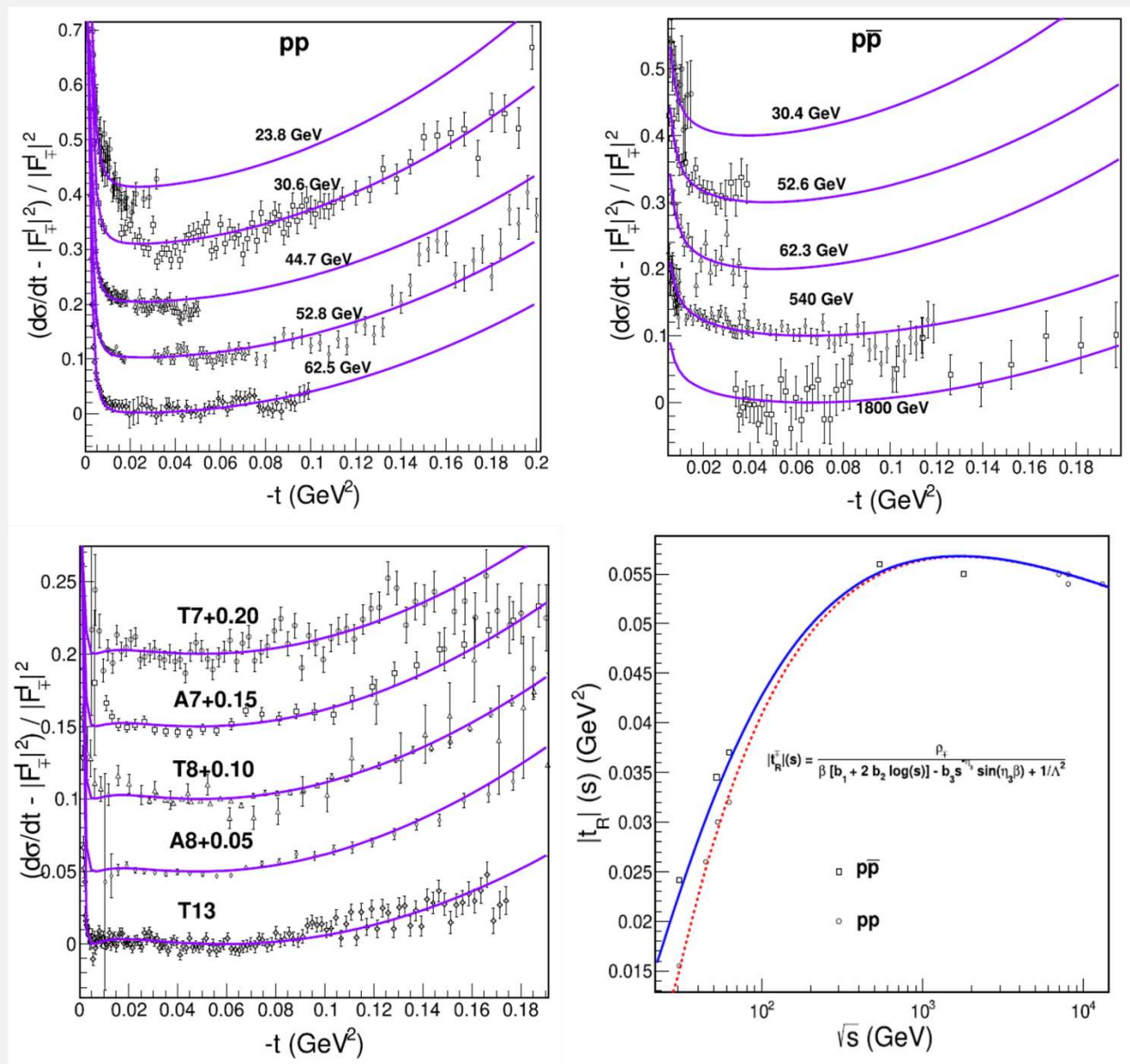
then, for s large, if $T_R^N(s, t) > |T_C(t)|$ in a region $0 < |t| < |t_R|$ then $T_R(s, t)$ has two zeros,

$$T_R(s, t_{\xi_1}) = T_R(s, t_{\xi_2}) = 0, \quad 0 < |t_{\xi_1}| < |t_{\xi_2}| < |t_R| \quad (9)$$

A.K.K, Eur. Phys. J. C 83 (2023) 2, 126

As the energy increases the real nuclear amplitude also increases



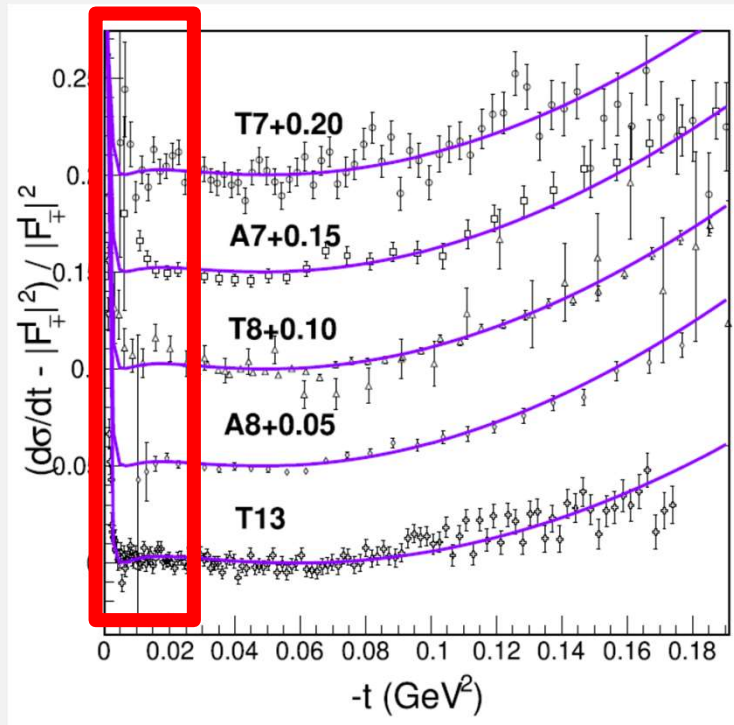


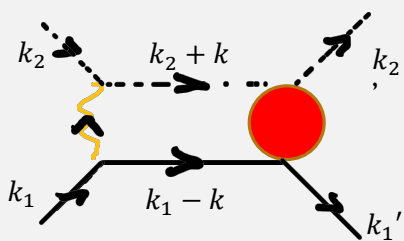
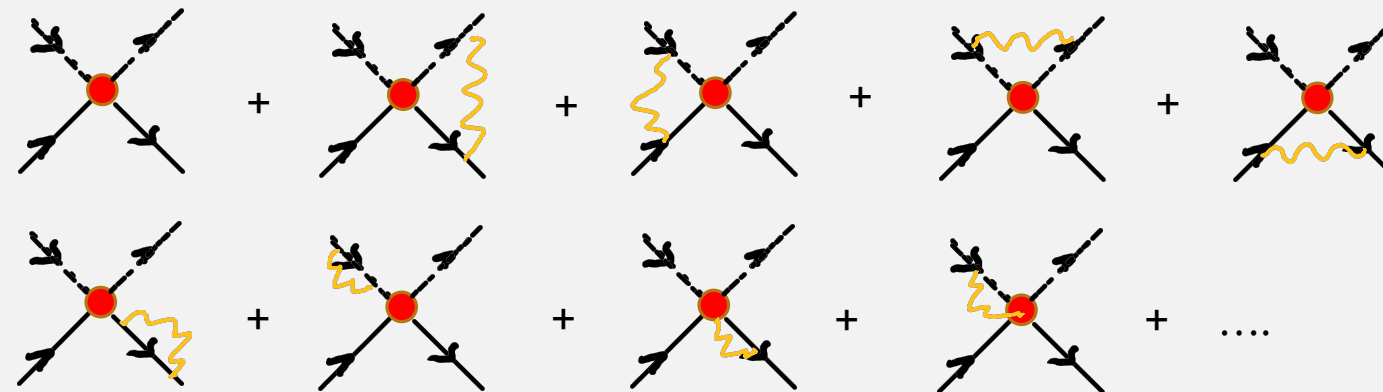
Analytic model for the very forward amplitudes

A.K.K., J.Phys.G 46 (2019) 12, 125001

$$T_R(s, t) + T_C(t) = 0$$

Is it possible to observe any dip due to the interplay between real and Coulomb amplitude?





$$I_N = -4\pi i \alpha (4k_1 \cdot k_2) \int \frac{d^4 k}{(2\pi)^4} \frac{f_N(2k_2 \cdot k + k^2, -2k_1 \cdot k + k^2, s, t')}{(k^2 + i\epsilon)[(k_2 + k)^2 - m^2 + i\epsilon][(k_1 - k)^2 - M^2 + i\epsilon]}$$

Similar results from adding Coulomb and Strong force eikonals R. Cahn, Z. Phys. C 15 (1982) 253.

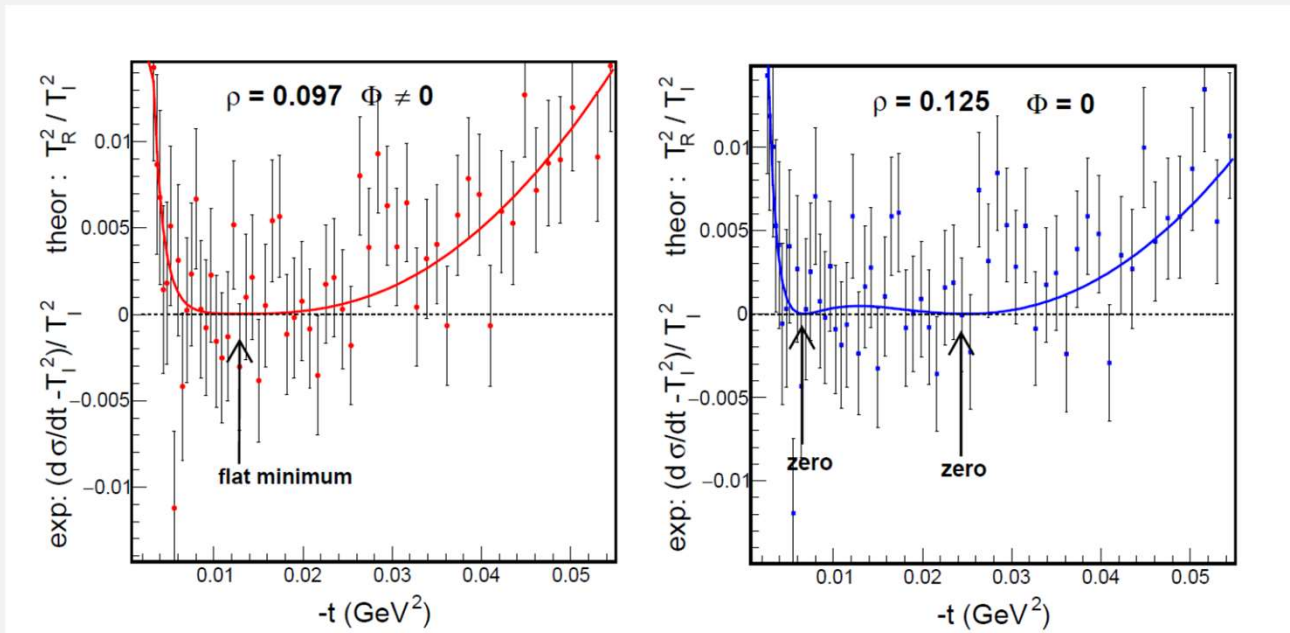
$$\left. \begin{aligned} T_{C+N}(s, t) &= \frac{s}{4\pi i} \int d^2 b e^{iq \cdot b} [e^{2i(\chi_c + \chi_N)} - 1] \\ T_C(t) &= \frac{s}{4\pi i} \int d^2 b e^{iq \cdot b} [e^{2i\chi_c} - 1] \\ T_N(s, t) &= \frac{s}{4\pi i} \int d^2 b e^{iq \cdot b} [e^{2i\chi_N} - 1] \end{aligned} \right\}$$

$$T_{C+N}(s, t) = T_C(t) + T_N(s, t) + \frac{s}{4\pi i} \int d^2 b e^{iq \cdot b} [e^{2i\chi_c} - 1][e^{2i\chi_N} - 1]$$

Relative Coulomb phase

$$\phi(s, t) = -\ln \left(\frac{-t}{s} \right) + \int_0^s \frac{dt'}{|t' - t|} \left[1 - \frac{F^N(s, t')}{F^N(s, t)} \right]$$

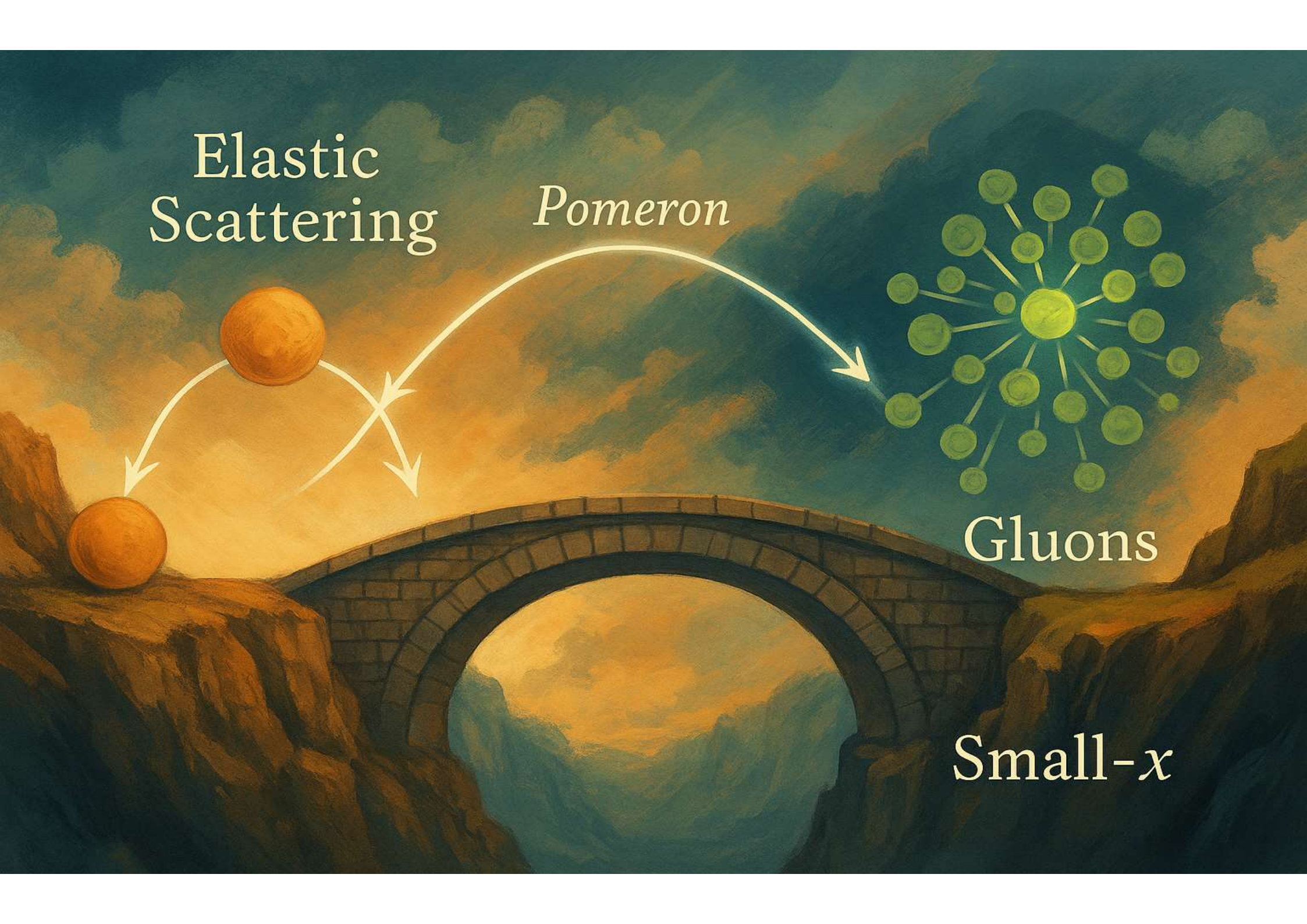
Explicitly $\phi(s, t) \sim -\left[\gamma + \ln\left(-\frac{Bt}{2}\right) + O(-Bt) \right]$



A.K.K., E. Ferreira and M. Rangel, Phys.Lett.B 789 (2019) 1-6

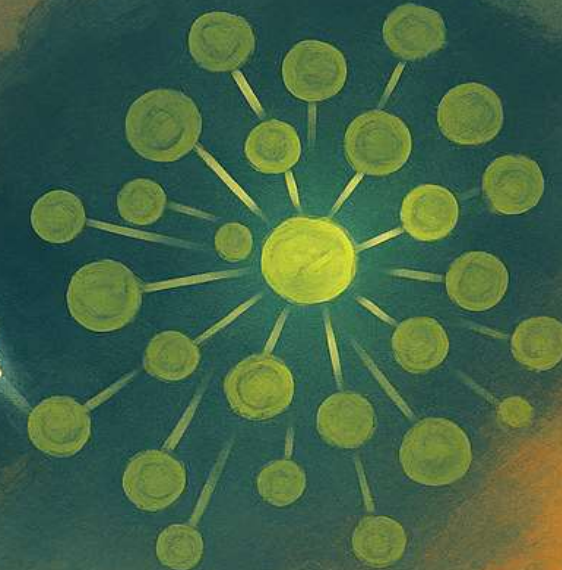
A.K.K., E. Ferreira, T. Kodama and M. Rangel, Eur.Phys.J.C 77 (2017) 12, 877

The presence of the Coulomb phase reduces the magnitude of ρ at LHC!

A landscape painting featuring a stone arch bridge spanning a river. In the background, there are rolling hills and mountains under a blue sky with white clouds.

Elastic
Scattering

Pomeron



Gluons

Small- x

feature	elastic scattering	small-x processes
typical process	$p+p \rightarrow p+p$	$e+p \rightarrow e'+X, \gamma^*+p \rightarrow V+p$, etc.
final state	only intact hadrons	inclusive or diffractive final states (may include jets, X)
kinematics	momentum transfer t	Bjorken- x $x \ll 1$, e.g. $x < 10^{-2}$
probed structure	hadronic form factor (impact-parameter space)	gluon density / unintegrated gluon distribution
parton picture	not explicit / soft physics	QCD partons (quarks, gluons), small- x dynamics
QCD regime	non-perturbative (soft)	perturbative QCD with high gluon densities
theoretical tools	Regge theory, eikonal models (... UP TO NOW)	DGLAP, BFKL, BK/JIMWLK, CGC
main observables	$d\sigma/dt$, total cross section	structure functions F_2 , F_L ; diffractive cross sections
experimental example	TOTEM (LHC), ISR, TEVATRON	HERA, LHCb (forward), UPCs at ALICE/ATLAS

Questions

- Can we describe any elastic scattering channel with our equation?
- Is the odderon an initial conditions problem?
- Is there diffusion in b -space?
- Is it possible to foreseen any asymptotic behaviour?
- Is the Coulomb phase really fundamental in charged hadrons?

For the future

- Use other models as initial conditions
- Extend the equation to different channels
- Use the hierarchy equations to study diffractive production
- Refine initial conditions to the real part
- Explore further connections between small-x and elastic scattering

"Entities must not be multiplied beyond necessity"



Illustration of William of Ockham (from Wikipedia)

Thank you!

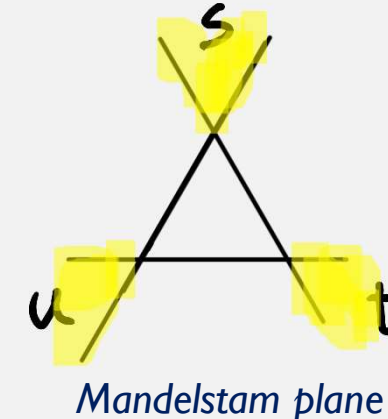
Assumptions

Analytic nuclear amplitude $A(s, t, u)$

Singularities have a physical meaning

Crossing symmetric amplitudes $A_{pp}(s, t, u) = A_{p\bar{p}}(u, t, s)$

Unitarity of S matrix $ss^\dagger = 1$



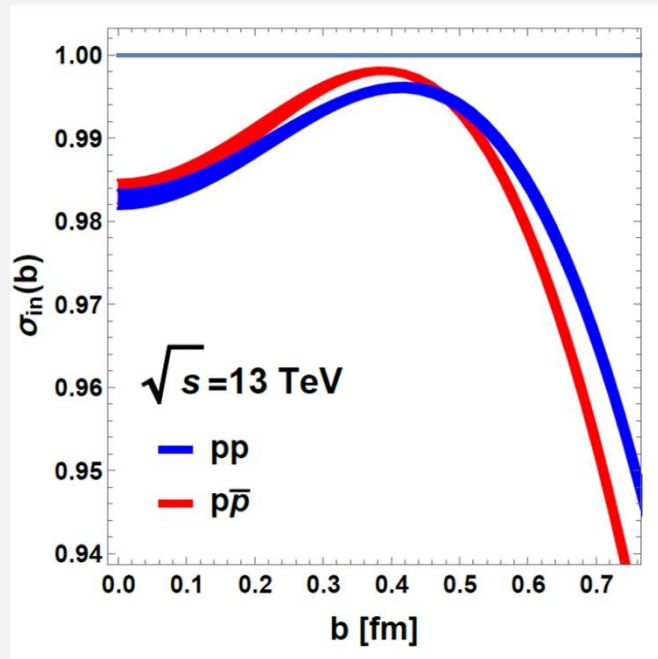
Theorems

Optical theorem $\sigma_T = \frac{1}{2|p|\sqrt{s}} \text{Im } A(s, t)$

Froissart theorem/bound $\sigma_T(s) \leq C \log^2 \left(\frac{s}{s_0} \right) \quad s \rightarrow \infty$

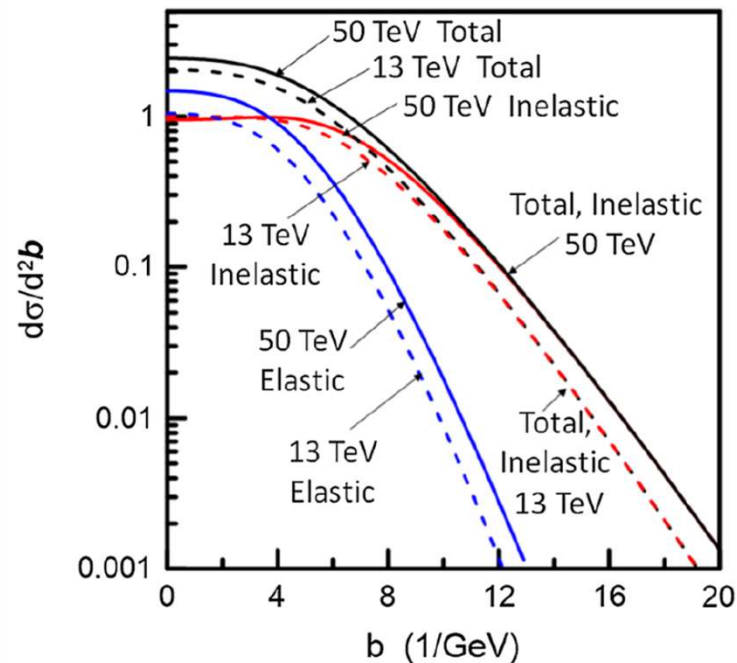
Pomeranchuk theorem $\frac{\sigma_T^{pp}(s)}{\sigma_T^{p\bar{p}}(s)} \rightarrow 1 \quad s \rightarrow \infty$

Something is going on at 13 TeV

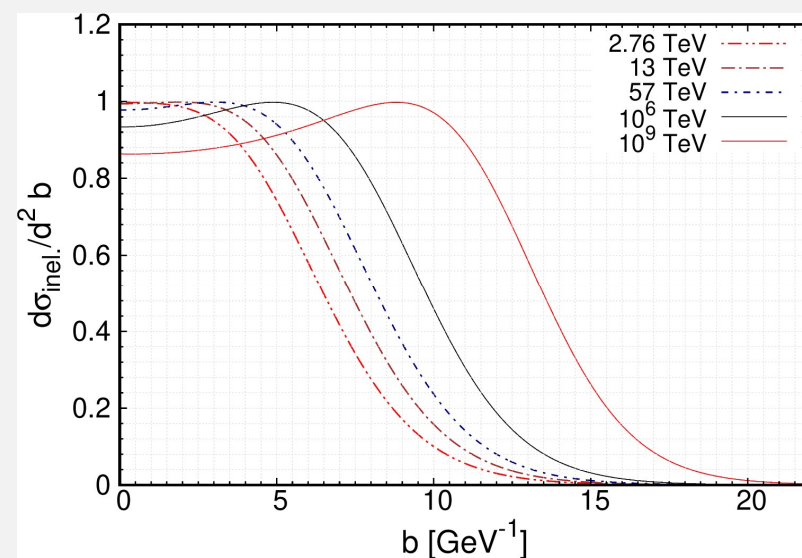


W. Broniowski, L. Jenkovszky, E. R. Arriola, I. Szanyi, *Phys. Rev. D* **98**, 074012 (2018); E. R. Arriola, W. Broniowski, *Few Body Syst.* **57** (2016) 7, 485-490; *Phys. Rev. D* **95** (2017) 7, 074030

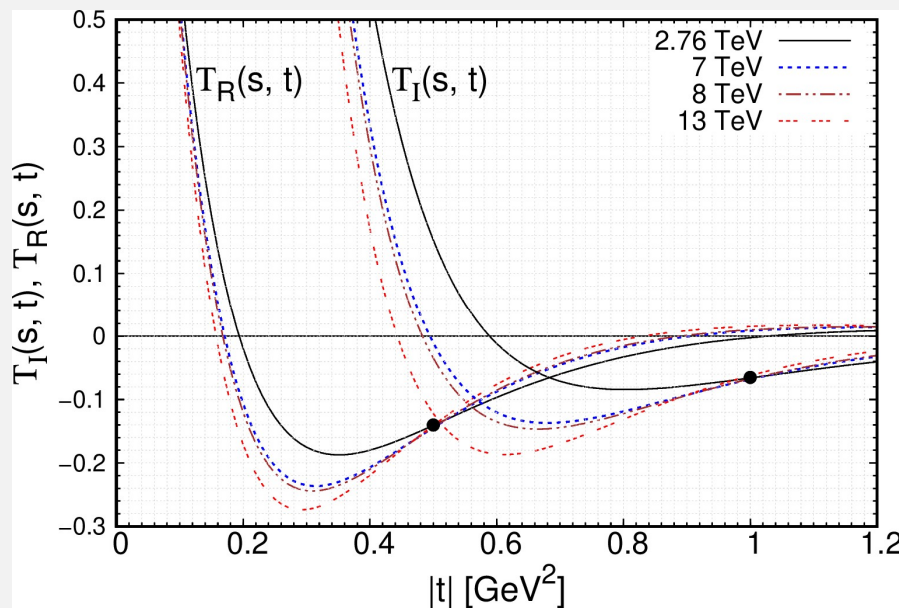
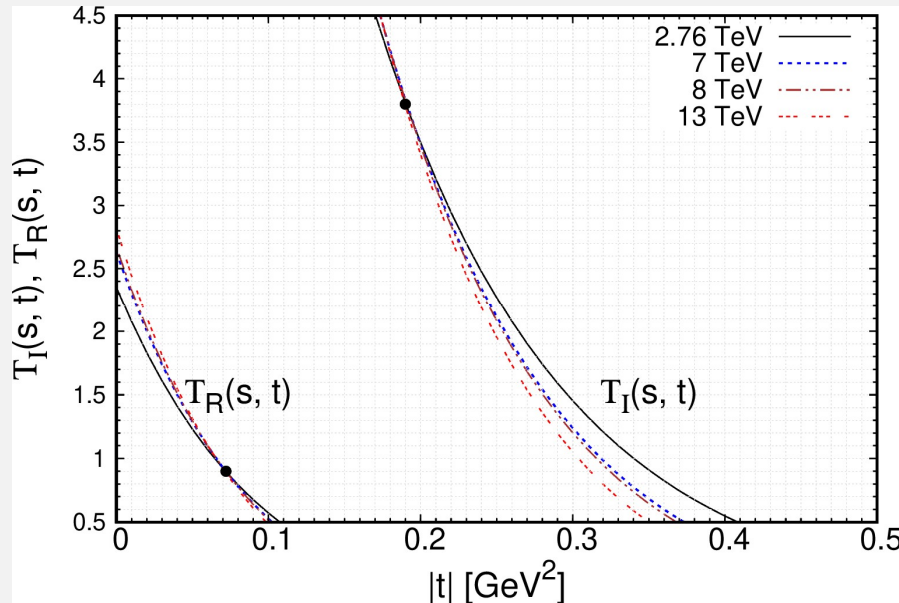
For LHC energies we also observe the ‘halo’ effect



E. Ferreira, A. K. K. and T. Kodama; *Eur. Phys. J. C* **81** (2021) 4, 290



The complex amplitudes in t-space are



We also observe stationary points in t-space.
This was observed by Csorgo et. al

*T. Csorgo and I. Szanyi, in International Scientific Days
- Femtoscopy Session (2022) <https://indico.cern.ch/event/1152630/>.*

BSW model

C. Bourrely, J. Soffer, and T. T. Wu, Phys. Rev. D 19, 3249 (1979)

eikonalized model

$$M(s, t) = \frac{is}{2\pi} \int d^2 b e^{-iq \cdot b} \left(1 - e^{-\Omega(s, b)} \right)$$

$$\Omega(s, b) = S(s)F(b) \quad \text{opacity}$$

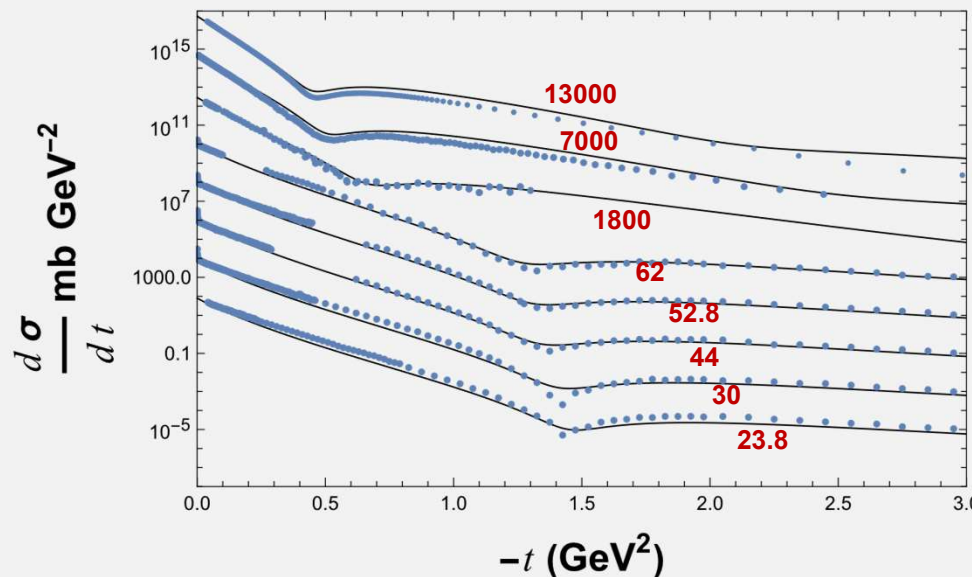
Symmetrized energy dependence $S(s) = \frac{s^c}{(\ln s)^{c'}} + \frac{u^c}{(\ln u)^{c'}}$ $F(b) = \frac{1}{2\pi} \int d^2 q e^{iq \cdot b} \tilde{F}(-q^2)$

with $\ln u = \ln s - i\pi$

Form factor

$$G(t) = \frac{1}{\left(1 - \frac{t}{m_1^2}\right)\left(1 - \frac{t}{m_2^2}\right)}$$

$$\tilde{F}(t) = f G^2(t) \frac{a^2 + t}{a^2 - t}$$



$c = 0.167$	$m_1 = 0.577 \text{ GeV}$	$a = 1.858 \text{ GeV}$
$c' = 0.748$	$m_1 = 1.719 \text{ GeV}$	$f = 6.971 \text{ GeV}^{-2}$

Parameters of the model

KFK model

A. K. K., E. Ferreira, and T. Kodama, Eur. Phys. J. C 74, 3175 (2014)

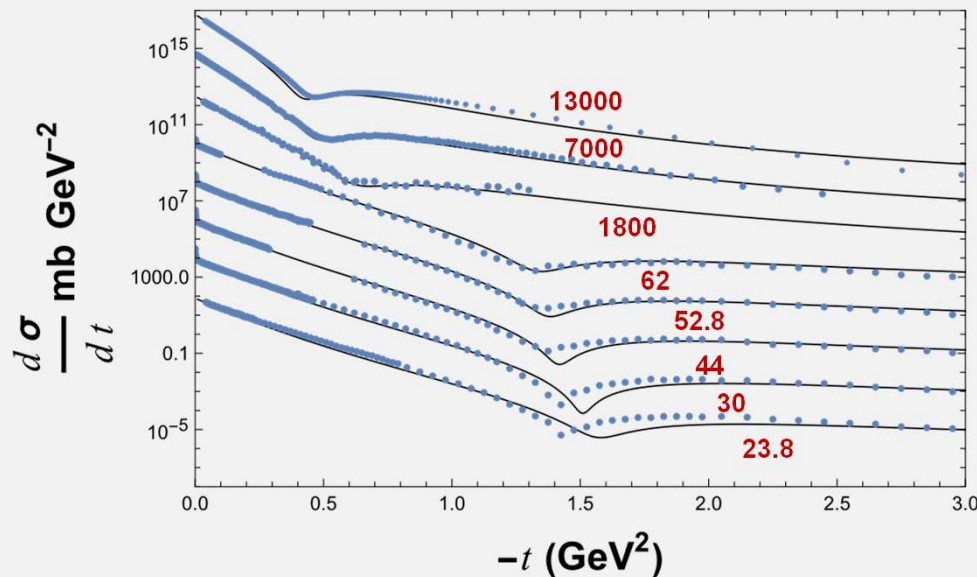
$$\widetilde{T}_k(s, b) = \frac{\alpha_k(s)}{2\beta_k(s)} e^{-\frac{b^2}{4\beta_k(s)}} + \lambda_k(s) \widetilde{\Psi}(s, b)$$

Based on Stochastic vacuum model

$$T_k(s, t) = \frac{1}{2\pi} \int d^2 b e^{-iq \cdot b} \widetilde{T}_k(s, b)$$

$$\widetilde{\Psi}_k(s, b) = \frac{2e^{\gamma_k(s) - \sqrt{\gamma_k(s) + \frac{b^2}{a_0}}}}{a_0 \sqrt{\gamma_k(s) + \frac{b^2}{a_0}}} \left[1 - e^{\gamma_k(s) - \sqrt{\gamma_k(s) + b^2/a_0}} \right]$$

Fourier transformation in closed forms in both t and b



Donnachie Landshoff model Pomeron exchange (Regge-like)

A. Donnachie and P.V. Landshoff, Physics Letters B 727 (2013)

$$\alpha_i(E) = 1 + \varepsilon_i + \alpha'_i t \quad i = P, \pm \quad \text{Regge trajectories}$$

One Pomeron, even and odd regge contributions

$$A(s, t) = -\frac{X_P F_P(t)}{2\nu} e^{-\frac{1}{2}i\pi\alpha_P(t)} (2\nu\alpha'_P)^{\alpha_P(t)} - \frac{X_+ F_+(t)}{2\nu} e^{-\frac{1}{2}i\pi\alpha_+(t)} (2\nu\alpha'_+)^{\alpha_+(t)} - i \frac{X_- F_-(t)}{2\nu} e^{-\frac{1}{2}i\pi\alpha_-(t)} (2\nu\alpha'_-)^{\alpha_-(t)}$$

Two Pomeron exchange (negative contribution)

$$\frac{X_P^2}{64\pi\nu} e^{-\frac{1}{2}i\pi\alpha_{PP}(t)} (2\nu\alpha'_P)^{\alpha_{PP}(t)} \left[\frac{A^2}{a/\alpha'_P + L} e^{\frac{1}{2}at} + \frac{(1-A)^2}{b/\alpha'_P + L} e^{\frac{1}{2}bt} \right]$$

“Perturbative” tri-gluon exchange

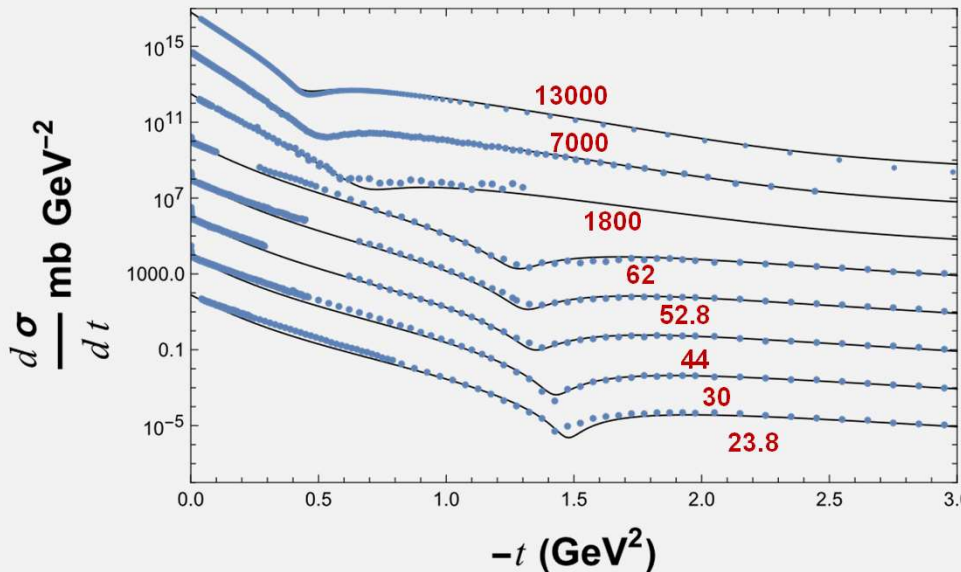
A. Donnachie and P. V. Landshoff, Phys.Lett. B387 (1996) 637-641

$$\frac{C}{t_0} e^{2\left(1-\frac{t^2}{t_0^2}\right)}$$

Form factor

$$F(t) = A e^{at} + (1-A) e^{bt}$$

$$L = \ln(2\nu\alpha'_P) - \frac{1}{2}i\pi$$



$\varepsilon_P = 0.110$	$\varepsilon_+ = -0.327$	$\varepsilon_- = -0.505$
$X_P = 339$	$X_+ = 212$	$X_- = 104$
$\alpha'_P = 0.165 \text{ GeV}^{-2}$	$a = 7.854 \text{ GeV}^{-2}$	$b = 2.470 \text{ GeV}^{-2}$
$A = 0.682$	$C = 0.0406$	$t_0 = 4.230 \text{ GeV}^{-2}$

Parameters of the model

Dynamical Gluon Mass model (QCD inspired)

E. G. S. Luna, A. F. Martini, M. J. Menon, A. Mihara, and A. A. Natale, Phys. Rev. D 72, 034019 (2005)

$$\text{Amplitude} \quad A(s, q^2) = \frac{i}{2\pi} \int d^2 b e^{-iq \cdot b} (1 - e^{i\chi_{pp}^{pp}(s, b)})$$

$$\text{Eikonal} \quad \chi_{pp}^{pp}(s, b) = \frac{i}{2} \left[\sigma_{qq}(s) W(b; \mu_{qq}) + \sigma_{qg}(s) W(b; \mu_{qg}) + \sigma_{gg}(s) W(b; \mu_{gg}) \pm k C_{odd} \frac{m_g}{\sqrt{s}} e^{\frac{i\pi}{4}} W(b; \mu_{odd}) \right]$$

Elementary cross sections

$$\sigma_{qq}(s) = k C_{qq} \frac{m_g}{\sqrt{s}} e^{\frac{i\pi}{4}}$$

$$\hat{\sigma}_{gg}(\hat{s}) = \left(\frac{3\pi_{\alpha_s}^{-2}}{\hat{s}} \right) \left[\frac{12\hat{s} - 55M_g^2\hat{s}^3 + 12M_g^4\hat{s}^2 + 66M_g^6\hat{s} - 8M_g^8}{4M_g^2\hat{s}[\hat{s} - M_g^2]^2} - 3 \ln \left(\frac{\hat{s} - 3M_g^2}{M_g^2} \right) \right]$$

$$\sigma_{qg}(s) = \left[C_{qg} + C_{qg}' \left[\ln \left(\frac{s}{m_g^2} \right) - i\frac{\pi}{2} \right] \right]$$

$$\sigma_{gg}(s) = C_{gg} \int_{4m_g^2/s}^1 d\tau F_{gg}(\tau) \hat{\sigma}_{gg}(\hat{s})$$

$$F_{gg}(\tau) = \int_\tau^1 \frac{dx}{x} g(x) g(\tau/x) \quad g(x) = N_g \frac{(1-x)^5}{x^{1+\epsilon}}$$

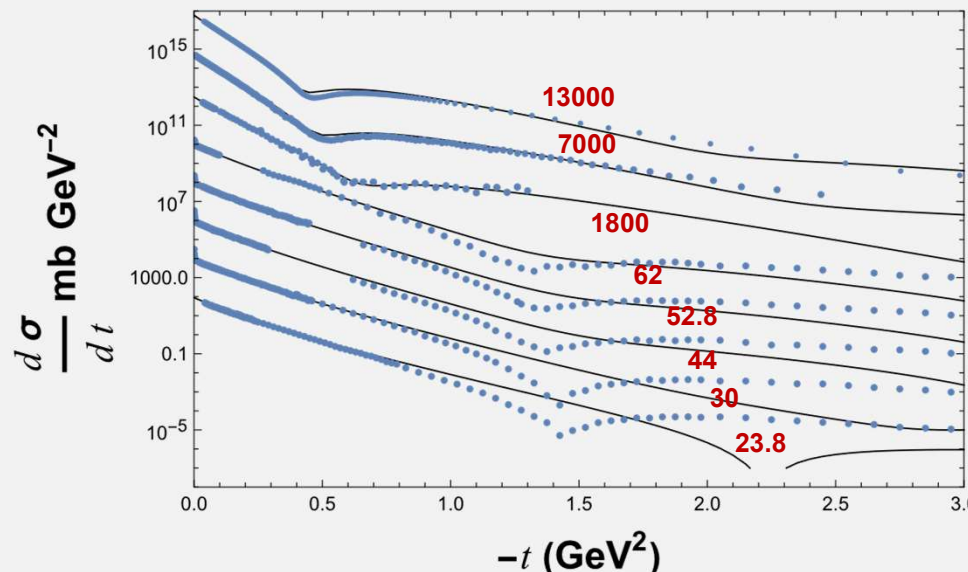
$$\text{b-profile} \quad W(b; \mu) = \frac{\mu^2}{96\pi} (\mu b)^3 k_3(\mu b)$$

running coupling

$$\bar{\alpha}_s(\hat{s}) = \frac{4\pi}{\beta_0 \ln \left[(\hat{s} + 4M_g^2(\hat{s}))/\Delta^2 \right]}$$

dynamic mass

$$M_g^2(\hat{s}) = m_g^2 \left[\frac{\ln \left[(\hat{s} + 4m_g^2)/\Delta^2 \right]}{\ln \left(4m_g^2/\Delta^2 \right)} \right]^{-12/11}$$



m_g	400 MeV
C_{odd}	3.03
C_{qq}	10.07
C_{qg}	0.874
C'_{qg}	0.0451
C_{gg}	0.00379
μ_{odd}	0.41
μ_{gg}	0.651
μ_{qq}	1.32
μ_{aa}	0.838

Jenkovszky model (reggeons +Pomeron+Odderon)

10

L.L. Jenkovszky, A.I. Lengyel, D.I. Lontkovsky, Int. J. Mod. Phys. A, 26, 4755 (2011)

Amplitudes $A(s, t)_{pp}^{p\bar{p}} = A_P(s, t) + A_f(s, t) \pm [A_\omega(s, t) + A_O(s, t)]$

trajectories

$$\alpha_k(t) = 1 + \delta_k + \alpha'_k t$$

$$A_R(s, t) = a_R e^{-\frac{i\pi}{2}\alpha_R(t)} e^{b_R t} \left(\frac{s}{s_0}\right)^{\alpha_R(t)}$$

reggeons

Energy dependence

$$r_1^2(s) = b_P + \ln(s/s_0) - \frac{i\pi}{2}$$

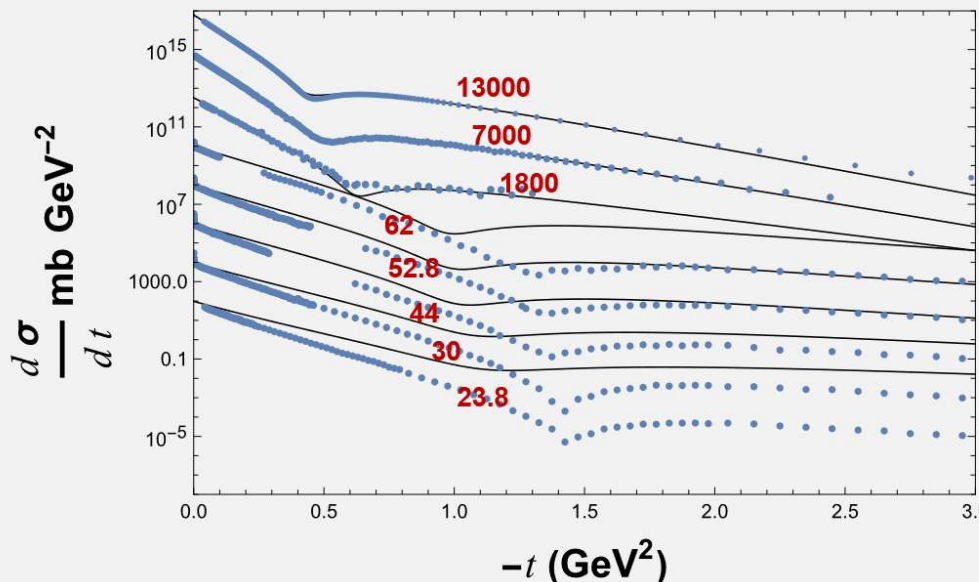
$$A_P(s, t) = i \frac{a_P s}{b_P s_0} \left[r_1^2(s) e^{r_1^2(s)[\alpha_P(t)-1]} - \varepsilon_P r_2^2(s) e^{r_2^2(s)[\alpha_P(t)-1]} \right]$$

Pomeron

$$r_2^2(s) = \ln(s/s_0) - \frac{i\pi}{2}$$

$$A_O(s, t) = \frac{a_O s}{b_O s_0} \left[r_{10}^2(s) e^{r_{10}^2(s)[\alpha_O(t)-1]} \right]$$

oddron



These curves are done with fixed parameters